# SUSTAINABLE INCORPORATION OF LIME-BENTONITE CLAY COMPOSITE FOR PRODUCTION OF ECO-FRIENDLY BRICKS

by

**USMAN JAVED**

(00000171071)

**Master of Science**

**in**

**Structural Engineering**

**NUST Institute of Civil Engineering (NICE)**
**School of Civil and Environmental Engineering (SCEE)**
**National University of Sciences and Technology (NUST)**
**Islamabad, Pakistan**
**(2019)**

This is to certify that the

thesis titled

**SUSTAINABLE INCORPORATION OF LIME-BENTONITE CLAY COMPOSITE FOR PRODUCTION OF ECO-FRIENDLY BRICKS**

submitted by

**USMAN JAVED**

(00000171071)

has been accepted towards the partial fulfillment
of the requirements for the degree

of

**MASTER OF SCIENCE**

**in**

**STRUCTURAL ENGINEERING**

_____

**Dr. Rao Arsalan Khushnood**

HoD Structural Engineering Department

NUST Institute of Civil Engineering (NICE)

School of Civil and Environmental Engineering (SCEE)

National University of Sciences and Technology (NUST), Islamabad,

Pakistan

## THESIS ACCEPTANCE CERTIFICATE

It is certified that Mr. Usman Javed, Registration No. 00000171071, of MS Structural Engineering batch 2016 has completed his thesis work and submitted final copy which was evaluated, and found to be completed in all aspect as per policy of NUST/Regulations. His thesis work was found to be free of plagiarism.

Signature: _____

Name of Supervisor/HoD: Dr. Rao Arsalan

Date: _____

Signature: _____

Dean: Dr. S. Muhammad Jamil

Date: _____

# DECLARATION

I certify that this research work titled "*Sustainable incorporation of lime-bentonite clay composite for production of eco-friendly bricks*" is my own work. The work has not been presented elsewhere for assessment. The material that has been used from other sources has been properly acknowledged /referred.

Signature of Student

USMAN JAVED

2016-NUST-MS-STR-00000171071

# COPYRIGHT STATEMENT

## ACKNOWLEDGEMENT

All thanks goes to Almighty Allah whose blessings gave me courage to undertake ability to accomplish this task. Indeed, it is He who guides us in every matter and renders His support.

I express my gratitude to my parents whose prayers and inspirational gestures always remained pivotal to my performance and achievements.

I am profusely thankful to my thesis supervisor Dr. Rao Arsalan Khushnood and co-supervisor Dr. Shazim Ali Memon for their productive advice, valuable guidance and kind supervision. I am also thankful to Dr. Ather Ali for his support and interest in this research. I also extend my thanks to staff of Structure and Combined(CASEN) Labs for their cooperation in availing SEM, XRD, TGA and FTIR testing facility.

Finally, I am indebted to my friends and colleagues especially Engr. Saeed Zafar, Engr. Tayyab Zafar, Engr. Mamoon Riaz, Engr. Muhammad Abubakar Tariq and Engr. Hamza Husnain for their valuable suggestions, experience sharing and ever ending moral support during my research work.

Dedicated

To

My Parents, Family, Teachers

And

Friends

# TABLE OF CONTENT

# LIST OF FIGURES

# LIST OF TABLES

# Abstract

Global earth atmosphere is degrading due to abundant use of fossil fuel for fulfilling energy demands of rapid growing economies. Brick manufacturing process contribute its part by consuming energy in its firing process, therefore, increase concentration of affluent greenhouse gasses and hazardous particulate matter, which causes global warming and cardio-respiratory diseases respectively. Therefore, proposed research aims to provide eco-friendly solution to the stated problems by incorporating locally available powdered lime-bentonite composite in compressed, unfired and fired clay brick. Characterization of lime, bentonite and its composite was determined individually by conducting scanning electron microscopy, X-ray diffraction, oxide composition, while gradation, atterberg limits and standard proctor test was conducted on composite level. Bricks for all three cases i.e. compressed, unfired and fired by replacing clay with 0, 5, 10, 15, 20% of bentonite keeping 5% quick lime constant. Bricks were then tested for compressive strength, flexure strength, unit weight, water absorption and thermal conductivity. Results indicated that calcium rich quick lime and silica rich bentonite being incorporated in clay brick decreased the $D_{50}$ values, increased the plasticity from low to higher values and decreased the values of optimum moisture content of lime-bentonite clay brick. Incorporation of lime-bentonite composite in compressed, unfired and fired bricks resulted increased compressive strength and flexure strength attributed to pozzolanic activity, decreased water absorption and unit weight due to swelling/healing property and enhanced microstructure by dissolution of silica and alumina to form calcium silicate hydrate and calcium aluminate hydrate. Strength gain of compressed bricks observed due to reduction in voids, pozzolanic activity, geo-polymerization reaction and interlocking of clay minerals, whereas, strength gain in fired bricks resulted due to bonding of micro sized clay minerals due to optimal sintering achieved at 1000°C. Thermal conductivity reduced from 0.51 to 0..38 resulting 15.45% reducing in cooling load and carbon foot prints for B20 compressed brick composite, which proved it an energy efficient and ecofriendly construction material. Corrosion resistance of compressed bricks increased from 0.72 to 0.81 with bentonite inclusion. Conclusively, lime-bentonite compressed clay bricks provides eco-friendly, energy efficient and sustainable options for production of green clay bricks.

# Chapter 1

# Introduction

## 1.1. General

Clay brick is an ancient construction material originated from Mesopotamia and Indus valley dates back around 10,000 years. According to archaeological evidence, clay the only constituent of ancient brick and type of sedimentary rock vastly found in Indus river valley (Roman, 2014). About 10,000 years ago, bricks were manufactured by sun-dry method, which was then fired by baking brick 10,000 and 5,000 years respectively before the discovery of Portland cement (Roman, 2014). Now a days, bricks are manufactured in kilns around 800C for36 hours (Syed M.S. Kazmi, 2016). Brick is one of the commonly used and oldest construction materials with worldwide production of about 1.391 trillion units of fired bricks per year reported in 2014 (Zhang, 2014). Pakistan is the third largest country contributing about 3%(59 billion) of the world's brick production with approximately 12,000 brick kiln (SAARC, 2012). Fired clay bricks gain their strength by sintering process, in which the crystalline mineralogical phases in clay get fused into the pores to densify the microstructure of fired brick(L. Vorrada, 2009). Energy consumption of fired clay brick is 2.0 kWh per unit by releasing 0.41 kg of $CO_2$ and particulate matter into the atmosphere during its manufacturing(Reddy BVV, 2003), which caused the progressive ecological degradation and global warming. However, several researchers enhanced the physico-mechanical properties of fired clay brick by incorporating various industrial waste and by-products in fired clay brick at their corresponding sintering temperatures (Haiying Z, 2011). Published literature reported the successful utilization of agro-industrial waste like municipal solid waste incinerated ash (Haiying Z, 2011), waste marble dust (Bilgin N, 2012), waelz slag and foundry sand (Quijorna N, 2012), dredged sediments (Mezencevova A, 2012), sugarcane bagasse ash (Faria KCP, 2012), rice husk ash (Rahman, 1987), petroleum effluent treatment plant sludge (Sengupta P, 2002) and paper processing residue (Sutcu M, 2009) as partial replacement of clay in fired bricks. Firing clay brick up to sintering temperature of incorporated crystalline phases for mechanical strength gain caused higher carbon foot print, greenhouse gasses and particulate matter in atmosphere due to consumption of low calorific valued fossil fuel, therefore, conventional brick firing process is energy intensive and eco-hazardous causes global warming and poses several health hazards.

Conventional clay brick manufacturing is energy intensive and eco-hazardous process which utilizes excessive energy, releases harmful gasses and particulate matter during firing process

(Roman, 2014; Shamiso Masuka, 2018). In Pakistan, coal is usually used to fire clay brick conventional kilns(Bull Trench Kilns) around 800°C temperature for 36 hours and then removed afterwards from kiln (Syed M.S. Kazmi, 2016). Moreover, according to survey conducted by SAARC (SAARC, 2012), brick kilns are also fired by low calorific valued bio-fuel like poultry litter, rice husk, sugarcane bagasse and sugar mill mud releasing several hazardous gasses.

Energy consumed during brick firing is associated with the global energy resource depletion, whereas, fossil fuel burning for fulfillment of energy needs disturbs global radiative balance and degrade atmosphere by affluent release of anthropogenic air pollutants including CO, $NO_x$, $SO_2$ etc., which accounted for several respiratory and cardiovascular diseases (Chen et al., 2017; Gao et al., 2003; Zhang et al., 2016). Whereas, world health organization (WHO) reported 3.7 million deaths (6.7% of total deaths) worldwide due to air pollution in 2012 (Lee et al., 2014). Moreover, global Earth's temperature increases by disturbing global radiative balance through backscattering and absorption of incident solar radiations(Gao et al., 2003). According to temperature analysis conducted by NASA's Goddard Institute for Space Studies (GISS), the average earth's temperature has increased 0.8°C between 1880 to 2017 (Robert Levy, 2017). The pictorial representation of increased global earth's temperature has been presented in fig. 2-1.

## 1.2. Problem Statement

Conventional fired clay brick manufacturing is energy intensive process evolve hazardous/carcinogenic gasses in atmosphere, therefore, government agencies and court has put ban on conventional brick kiln. The increasing demand of clay brick for construction industry can be meet by introducing new technique of brick manufacturing. In this regards, lime-bentonite clay composite was evaluated for compressed, fired and unfired clay bricks.

## 1.3. Significance

1. To investigate suitability of lime bentonite clay composite as partial replacement of brick clay by characterization.
2. To examine the mechanical, microstructural and durability properties of lime bentonite clay composite
3. To estimate the efficiency of in terms of thermal insulation and conservation of brick firing energy

## 1.4. Scope

Factors that remain constant throughout the mixes are:

1. Lime Content was kept constant, whereas water content used was plastic limit and OMC for uncompressed and compressed bricks respectively.
2. Bentonite and clay content increased and decreased respectively.

Parameters vary for different mixes are:

Bentonite to clay ratio changes at different replacements percentages (0:100, 5:95, 10:90, 15:85, 20:80) %.

## Chapter 2

# Literature Review

### 2.1. General

Many researchers have investigated the potential use of geo-polymerization reaction for reducing firing energy and potential environmental degradation during bricks firing process (Chen C, 2012). Natural chemical reaction between amorphous silica and alumina rich powdered minerals occurred in concentrated silicate and hydroxide solution at ambient or elevated temperature to constitute a stable alumino-silicate called geo-polymer by involved chemical reaction known as 'Geo-Polymerization'. Several agro-industrial wastes such as bottom ash(Chen C, 2012), fly ash (Arioz O, 2010; Freidin, 2007; Kumar A, 2013), rice hush ash (Mohan NV, 2012), copper mine tailing (Ahmari S, 2012) and slag have been utilized to enhance the mechanical and microstructural properties of unfired bricks through geo-polymerization.

### 2.2. Synergism of Hydration and Pozzolanic Reaction

Calcium hydroxide is by-product of hydration reaction, which is most susceptible to a chemical attack and do not plays role in strength development of concrete. High calcium hydroxide content presence account for chemical attack. However, as the porosity and permeability decrease with more bentonite percentage replacement, the mixture becomes sounder and less permeable due to pozzolanic reaction (Adesanya and Raheem, 2010).

Hydration Reaction (Neville 2000):-

$$3C_3S + 6H \longrightarrow C_3S_2H_3 + 3Ca(OH)_2$$

$$2C_2S + 4H \longrightarrow C_3S_2H_3 + Ca(OH)_2$$

$C_3S$ ---------- Tri-calcium silicate

$C_2S$ ---------- Di-calcium silicate

$C_3S_2H_3$ ---------- Calcium silicate hydrate (CSH)

Pozzolanic reaction (Mehta 2006):

$$\text{Pozzolan} + Ca(OH)_2 + H \longrightarrow C_3S_2H_3$$

Previous studies have indicated that up to 20% ground pozzolan may be advantageously blended into the mixture without adversely affecting the strength and durability of the resulting concrete (Nehdi M, 2003). In addition, it is possible to use residual agricultural waste ash without grinding by adapting the mixing process to optimize the ash particle size (Zain MFM, 2011).

Published literature has revealed that properties like compressive strength, chlorine ingress, sulphate attack, and other durability aspects are the functions of micro-ingredients present in cement concrete and are accessed and stimulated by use of pozzolans in concrete. Water to cement ratio plays a key role to ensure durability and strength of concrete. More the w/c will be more will be the bleeding and more non-uniform will be the mix. Use of finer material can decrease effective water cement ratio by increasing water demand, hence decrease the problems related bleeding. Cement concentration usually at the top surface (formation of Laitance) will be more than any other part below it. That causes segregation of the cement particles from other ingredients. Due to which permeability increases and concrete would be more susceptible to sulphate attack, chlorine penetration, acid attack, alkali silica reaction and other durability issues. That is the main problem concrete gains enough initial strength but relatively lesser prolonged strength. However, it is concluded that sustainable concrete was not possible unless supplementary cementing materials of higher surface area and of more pozzolanic activity, like silica fume is used (Raut S, 20013). Moreover, aggregate take part in carrying major portion of stresses in concrete, their gradation, size, shape and geological formation are of great concern (Nehdi M, 2003).

By the use of pozzolan as cement blended material, the properties of concrete enhanced due to effect of above mentioned aspects. Then use of pozzolanic material as fine aggregate replacement would be beneficial manifold for concrete properties. Such waste materials have used in concrete as fine aggregate replacement that are discussed as follow.

### 2.3. Geo-polymerization

Lime stabilization for improving soil stiffness and mechanical strength in elongated time is evident in literature for centuries (Bell, 1996; Brandl, 1981; Glenn, 1963; Sudhakar Rao, 2005.; Tremblay, 2001). Quick lime addition to clay-water system initiate an exothermic reaction evolving $17x10^9$ J of heat inducing high plasticity to the clay due to water evaporation, flocculation of mineral particles caused by ion formation($Ca^{2+}$, $OH^-$) and hydration of quick lime, whereas, long-term strength development is associated with the solidification due to the pozzolanic reaction (Boardman, 2001). Highly saline environment after lime hydration

dissolve alumino-silicate minerals present in clay, in which $Ca^{2+}$ ions react with the clay minerals to form calcium silicate hydrate (CSH) and Calcium aluminate hydrate(CAH) (Sherwood, 1993). These amorphous hydration phases crystallizes with time producing pozzolanic products bonding clay particles(Bell, 1996; Ingles, 1972; James, 2008; Little, 1996). Several researchers investigated the elongated pozzolanic reaction involved between lime treated bentonite and clay minerals. Vitale et. al. (E. Vitale 2017) examined the time evolution of pozzolanic potential of lime treated kaolinite and bentonite. Results indicated that the lime treated kaolinite exhibit slower pozzolanic reaction due to coating of adsorbed portlandite on its surface(E. Vitale 2017), whereas lime treated bentonite showed higher pozzolanic activity by consuming portlandite in faster rate attributed toward its higher surface area and high ion exchange capability of montmorillonite (Boardman, 2001; E. Vitale 2017).

Therefore, current research has been focused on reducing fired energy and effluent release of hazardous pollutants (which degrade atmosphere and cause several diseases) during conventional brick manufacturing. Physico-mechanical properties of clay brick can be enhanced by lime stabilization along varying replacement percentages of bentonite replaced clay composite. Mixing water content, particle size, oxide composition, material morphology, microstructure and crystallographic nature of phases present were determined in characterization studies for suitable incorporation of the lime bentonite composite in clay brick, whereas, compressive strength, flexure strength, water absorption and thermal conductivity was conducted evaluating physico-mechanical properties. Microstructural analysis included Fourier Transform Infrared Spectroscopy(FTIR), X-ray diffraction(XRD) and Thermogravimetric analysis(TGA) of compressed and unfired bricks were conducted at elongated curing age to study the contribution of hydration and pozzolanic reaction in strength gain. Comparison was developed for compressed, fired and unfired bricks, whereas one of the optimum brick types was selected with better results based on above physico-mechanical, durability and microstructural investigations. Lastly, energy efficiency and associated carbon emission for cooling load of prototype room built with optimum brick type(compressed) was determined. However, this research for the first time investigates the physico-mechanical, durability, energy efficiency and carbon emissions of incorporated bentonite in lime stabilized compressed clay bricks.

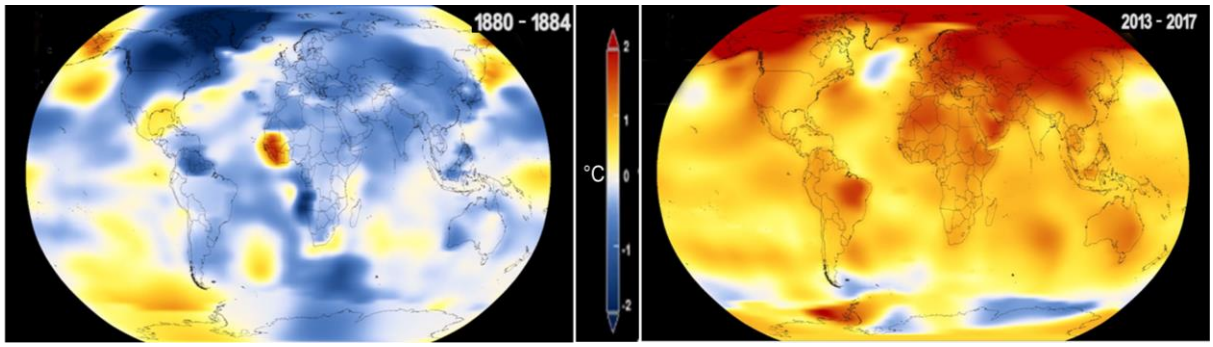


Figure 2-1: Global increase in earth temperature between 1880 and 2017[Source:(Robert Levy, 2017)]

# Chapter 3

# Experimental Investigation

## 3.1. Raw Materials

Natural clayey soil, powdered lime and bentonite were used in this research for manufacturing of bricks. Clay was obtained from brick kiln, whereas quick lime used was taken from industrial estate Hattar, Taxila. Sodium bentonite being characterized by high swelling and healing characteristics was acquired from mining site at Chandan Ghari District Peshawar, Pakistan.

## 3.2. Characterization

Macro and microscopic characterization of lime, bentonite, and clay was performed on both individual and composite levels. Oxide composition of clay, bentonite and quick lime was determined by X-ray fluorescence is shown in Table 1. The abundant presence of silica and alumina observed in clay(soil) along fewer proportions of oxides of iron, calcium and magnesium. However, cumulative proportions of silica, aluminum and iron oxides determined as 88.02% and the concentration of calcium, magnesium, potassium, iron and titanium oxides are greater than 9% with calcium oxide content greater than 6%. Therefore, according to Maniatis and Tite (A. Mohamed Musthafa, 2010; Y. Maniatis, 1981) the used clay characterized as low refractory calcareous, whereas, the concentration of silica exists between 50-60% and iron oxide more than 3%, therefore, satisfied the suitable chemical composition as reported in literature (A. Mohamed Musthafa, 2010). However, quick lime used in this study was primarily composed of calcium oxide(91.51%) and fewer concentration of silica(9.49%) along average particle size of 1 µm. Oxide composition of bentonite has shown silica, alumina and iron as major constituents with cumulative value of 91.73% with average particle size of 10 µm satisfying ASTM C618(ASTM., 2017) requirement for a pozzolan. Mineralogical nature of lime and bentonite was determined by X-ray diffraction using diffractometer model JDX-3532 JEOL, Japan with 2θ scan between 20°-70° ash shown in fig. 2. “MATCH Phase Identification v3.0” software interface was used to identify the diffraction peaks of chemical phases using ICDD. According to published literature, phase diffraction peaks intensities are proportion to the component producing it and difference among the peaks symbolizes the difference among concentration of the components(Stutzxnan, 1995). For quick lime, diffraction peaks of calcium oxide was observed at 28.83°(d=3.09Å), 33.97°(d=2.63Å), 47.55°(d=1.91 Å), 51.01°(d=1.78 Å) and 54.71°(d=1.67Å). Phases identified for bentonite were quartz, montmorillonite and kaolinite. Quartz identified at 2θ

phase diffraction angles of 22.39°(d=3.96Å), 27.79°(d=3.20Å), 36.48°(d=2.46Å), whereas montmorillonite and kaolinite identified at 24.06°(d=3.69 Å), 35.71°(d=2.51 Å), 61.77°(d=1.50 Å) and 30.67(d=2.91Å) respectively. Scanning electron microscopy(SEM) of the lime and bentonite was conducted using model JSM-5910 JEOL, Japan. SEM micrograph of lime and bentonite are shown in figure 3 revealed the morphology, texture and size of particles. The sequential magnified images of lime and bentonite at both macro-micro level has been shown in in figure 3(a-d) and (e-f) respectively. The variation among the particle sizes of lime and bentonite exists between the range of 2-15µm and 1-150µm respectively. Crystalline surface of lime, whereas smooth and angular surface of bentonite particles were observed with fragmented 1µm sized particles being attached on the surface of the larger particles. Energy dispersive spectroscopy of the micrograph revealed that the quick lime contain highest concentration of calcium oxide and that of bentonite powder contain the greatest concentration of silica as shown in fig. 3. Lime-bentonite composites containing 0, 5, 10, 15 and 20% of bentonite as clay replacement and constant (5%) concentration of lime was designated as CM, B05, B10, B15 and B20 respectively. The average particle size ($D_{50}$) of CM, B05, B10, B15, and B20 composites were recorded as 0.71, 0.40, 0.35, 0.31, and 0.27 mm respectively as per ASTM standard specification D7928 (ASTM, 2017a). The reduction in average particle size of the composites along bentonite replacement is due to the finer particle size of bentonite comparative to clay particles. Unified soil classification system(USCS) of clay classified 'CL' as clayey soil with low plasticity, which was then altered to intermediate and 'CH' higher plasticity inorganic clays for B05, B10 and B1, B20 composites respectively as shown in fig 5. Atterburg limits of lime bentonite clay composite was determined as per(ASTM, 2017b), to identify the plastic behavior and consistency of fine grained soil containing lime-bentonite clay composite. The result indicated that clayey soil with low plasticity was used, which was then transformed into intermediate and higher plasticity lime-bentonite clay composites values upon bentonite replacement due to presence of higher silica content attribute the plasticity and mixture hardness respectively (Kae Long Lin, 2006). Liquid and plastic limit values for the composites were recorded for CM, B05,B10, B15 and B20 as 28.64, 42.85, 48.50, 73.62, 80.76% and 22.72, 34.99, 40.09, 44.84, 56.175% respectively. The regression relation for liquid limit(L.L) and plastic limit(P.L) was determined as $L.L = 23.325e^{0.2645(\% \text{ Bent.})}$ and $P.L = 21.812e^{0.1875((\% \text{ Bent.})}$ being mentioned in fig. 7. Maximum molding density of compressed bricks was desired to achieve for all composite mixes which was determined by standard proctor test as per British Standards BS 1924-2 (Institute, 1990). OMC values for CM, B05, B10, B15, and B20 were recorded as 18.21, 22.68,

25.32, 31.39, 31.39% respectively as shown in fig.8. The polynomial regression equation for dry density curves is $y = 3.0007x^2-158.99x+4014.7$ with correlation coefficient value(R) of 0.99 shows the good relation between data points and the curve. Both optimum moisture content(OMC) and Atterberg limit values of the composites containing higher proportion of bentonite increased due to bentonite's higher affinity for water being absorbed in interlayer and ionic exchange potential (Oti, 2010). Therefore, compressed bricks were casted at OMC, while unfired and fired bricks were casted at the values of their plastic limits of the composites.

### 3.3. Preparation of bricks

Powdered clay, bentonite, and lime were manually dry mixed in proportions mentioned in Table 2. Bentonite was used to replace 0, 5, 10, 15, 20 % of clay designating the composites CM, B05, B10, B15, B20 respectively, keeping the 5% lime content constant throughout all composites. After the dry mixing being carried out, both compressed and normal bricks were mixed separately at corresponding plastic limits and optimum moisture content respectively of lime-bentonite composites as shown in fig. 7 & 8 respectively. Compressed bricks were compressed at molding pressure of 5 MPa and normal bricks were manually hand molded to produce 9x4.5x3in sized green bricks. Compressed bricks were moist cure at 25±3°C and relative humidity of 90% for 60 days. Normal molded bricks were sun dried for a month to evaporate moisture, so to avoid shrinkage cracks due to sudden and excessive loss of moisture at firing stage (Surendra Roy, 2007). Sundried bricks were then fired in electric furnace at peak temperature of 800 and 1000°C with the increase in temperature of 10 and 15°C/minute respectively as shown in figure 8 to avoid thermal stresses(X. Lingling, 2004). The fired samples were cooled through natural convection process by exposing the samples to room temperature. The sundry, fired and compressed bricks were subjected to series of physico-mechanical, thermal conductivity and microstructural investigations.

### 3.4. Test Methodology

Compressive strength, water absorption, unit weight was determined as per standard specifications of ASTM C67. Thermal conductivity of AAC was assessed in accordance to ASTM C177 (ASTM C177-13). Microstructural analysis involved Scanning Electron Microscopy(SEM), Fourier transform infrared spectroscopy(FTIR), X-ray diffraction(XRD) and thermogravimetric analysis(TGA) of compressed and unfired compressed bricks were conducted at 90 curing age to study hydration phases and the contribution of chemical/pozzolanic reaction involved in strength gain. Fourier transform infrared spectrometer(Perkin Elmer Spectrum 100) aided with universal attenuated total

reflection(ATR) assessory was used to identify the bonds vibration of hydration phases of compressed lime-bentonite clay bricks in transmission mode between frequency range of 4000-550° $cm^{-1}$ with spectral resolution of $4cm^{-1}$. Thermo-gravimetric analysis of AAC was conducted using 10x10mm concrete chunks which were soaked in acetone for stopping hydration at 90 days of curing age as mentioned in 'Lea's Chemistry of Cement and Concrete' (Hewlett, 2003). Scanning Electron Microscopy(SEM) aided with Energy Dispersive X-ray Spectroscopy (EDX) of compressed bricks samples were conducted to examine the morphology, pore sizes and hydration products of lime-bentonite incorporated compressed bricks. Comparison developed for compressed, fired and unfired bricks, whereas one of the optimum brick types(compressed brick) selected with better results based on above physico-mechanical and microstructural properties. However, energy efficiency and associated carbon emission for cooling load for prototype room built with optimum brick type was determined to ensure the energy conservation and environment protection. Durability evaluates the performance of bricks in acid rain being caused by nitric oxide and sulphur dioxide evolved from industries (Roger J. Cheng, 1987). Compressed bricks samples at varying bentonite content were immersed in 2% sulphuric acid solution for 28 days. Corrosion resistance of compressed bricks was calculated using following equations(Alaa A. Shakir, 2013).

$$W.G = \frac{W2-W1}{W1} \qquad (1)$$

W.G: Weight gain ratio

$W_1$: Brick weight before immersion in sulphuric acid

$W_2$ : Brick weight after immersion in sulphuric acid

Corrosion resistance of compressed bricks can be calculated as equation as following(M. Shahul Hameed, 2009).

$$P.C.R = \frac{\sigma a}{\sigma n} x100 \qquad (2)$$

P.C.R: Percentage corrosion resistance

$\sigma_a$ : Compressive strength of compressed brick immersed in acid

$\sigma_n$: Compressive strength of normal compressed brick

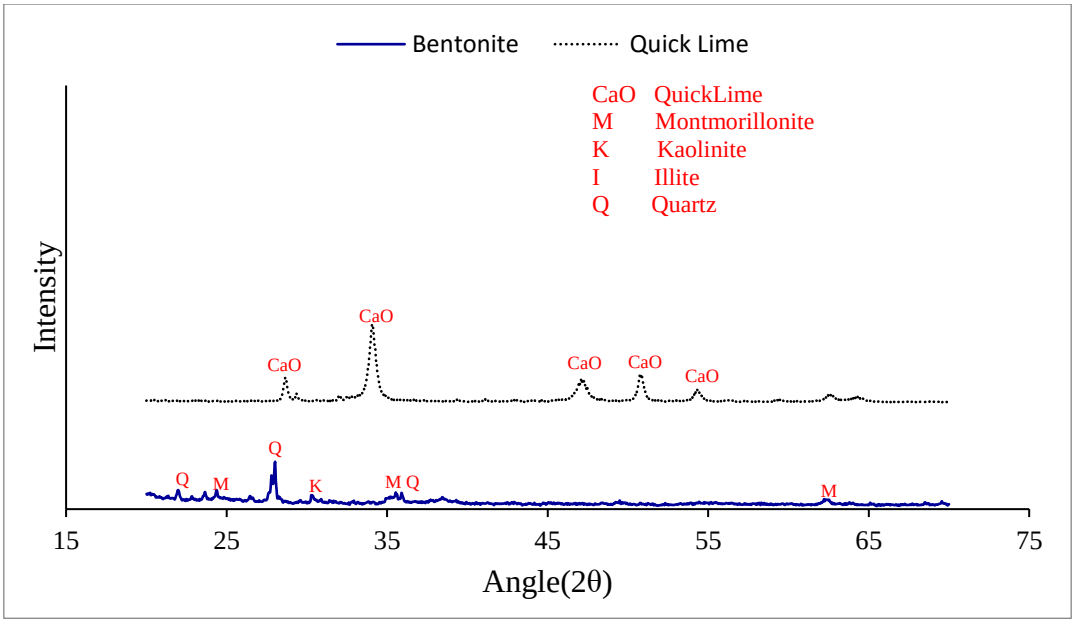


Figure 3-1:X-Ray Diffraction of bentonite and quick lime

Table 3-1: X-Ray Fluorescence of clay, bentonite and quick lime

| Oxide Composition | Clay | Bentonite | Quick lime |
|---|---|---|---|
| $SiO_2$ | 66.27 | 63.74 | 8.49 |
| CaO | 6.47 | 1.38 | 91.51 |
| $Al_2O_3$ | 18.34 | 24.53 | - |
| $Na_2O$ | 0.55 | 1.64 | - |
| MgO | 4.43 | 2.49 | - |
| $Fe_2O_3$ | 3.41 | 5.46 | - |
| $K_2O$ | 0.43 | 0.53 | - |
| $P_2O_5$ | 0.07 | - | - |
| MnO | 0.03 | - | - |
| $TiO_2$ | - | 0.23 | - |
| LOI | 8.31 | 9.65 | 5.67 |

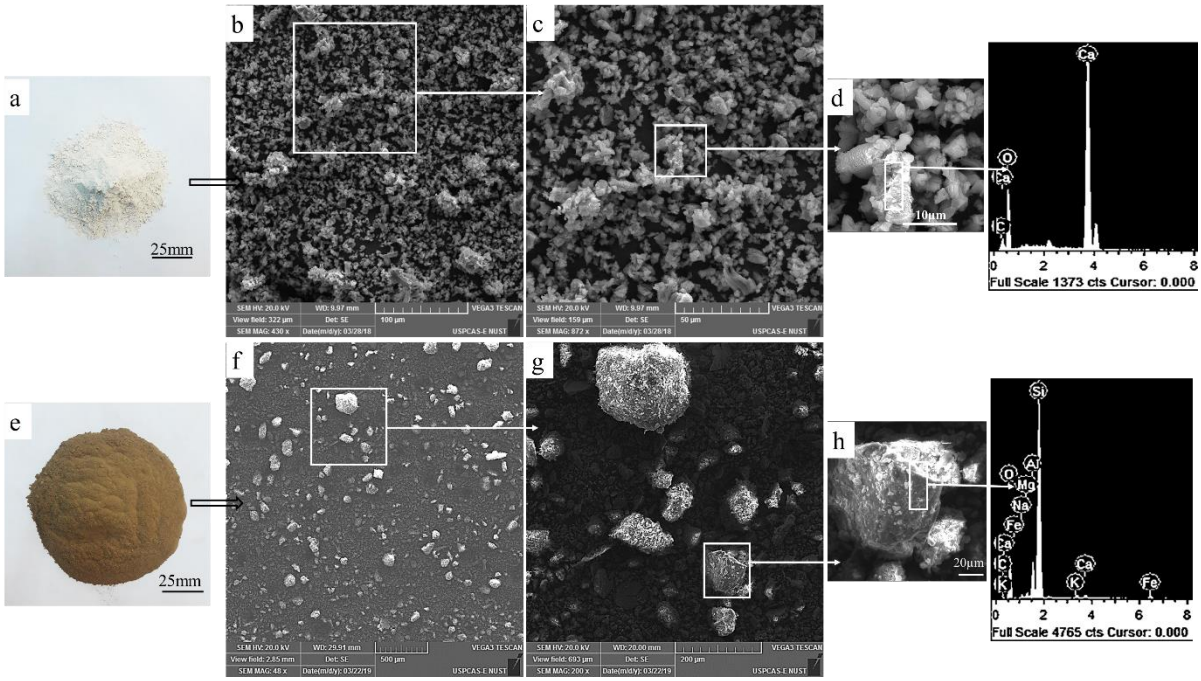


Figure 3-2: SEM and EDX of quick lime(a-d) and bentonite(e-h) powder

Table 3-2: Mix composition of lime-bentonite composite

| Mix Designation | Mix Composition(Percent by weight) | | | | |
|---|---|---|---|---|---|
| | Clay | Lime | Bentonite | Water(Plastic Limit) (For unfired, Fired bricks) | Water(OMC) (For compressed bricks) |
| CM(Control) | 95 | 5 | 0 | 22.72 | 18.21 |
| B05 | 90 | 5 | 5 | 37.09 | 22.68 |
| B10 | 85 | 5 | 10 | 41.19 | 24.52 |
| B15 | 80 | 5 | 15 | 44.84 | 28.62 |
| B20 | 75 | 5 | 20 | 52.77 | 28.62 |

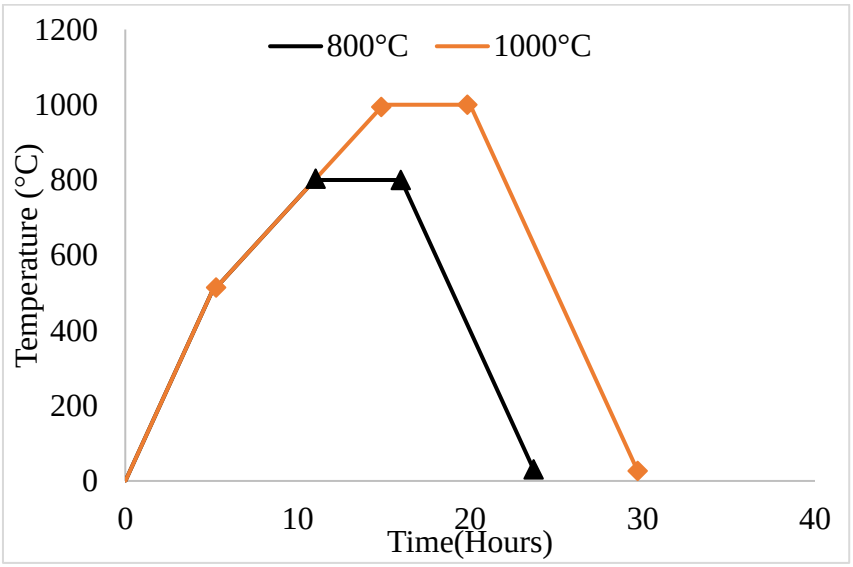


Figure 3-3: Firing regime of lime-bentonite clay bricks fired at 800 and 1000°C

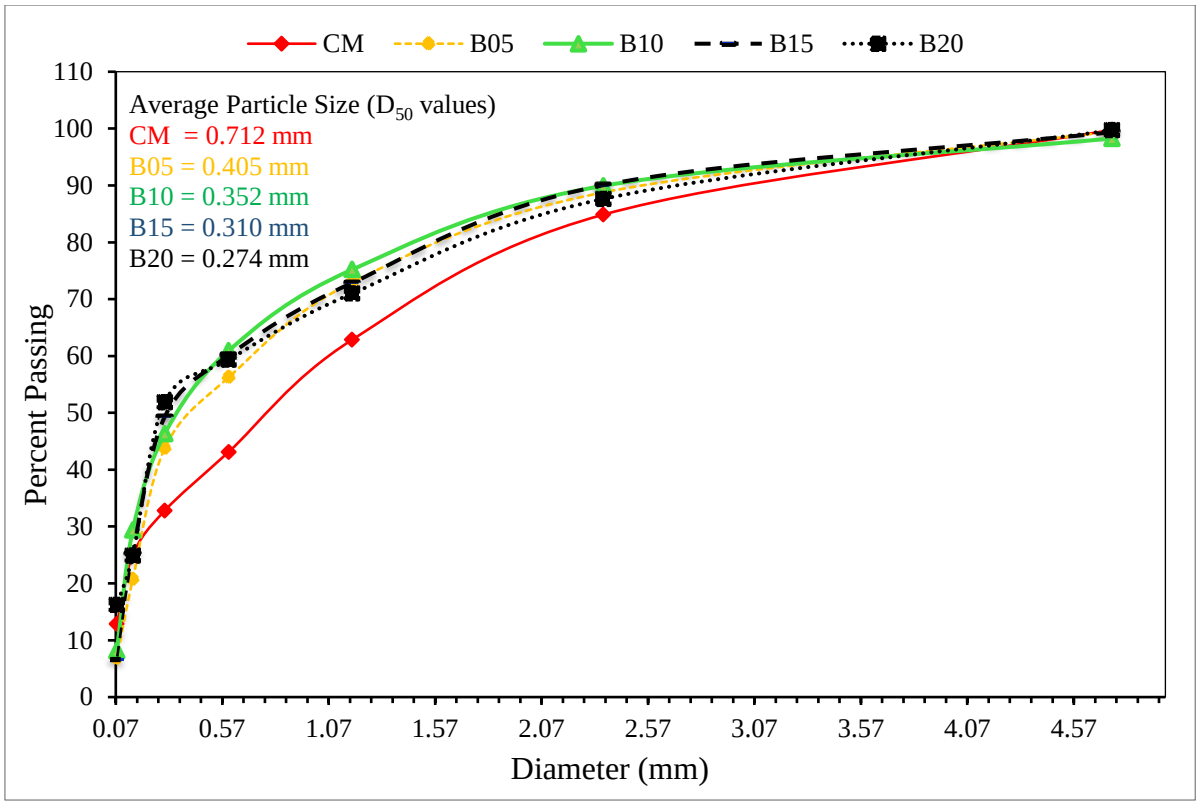


Figure 3-4: Particle size analysis of lime-bentonite clays composites

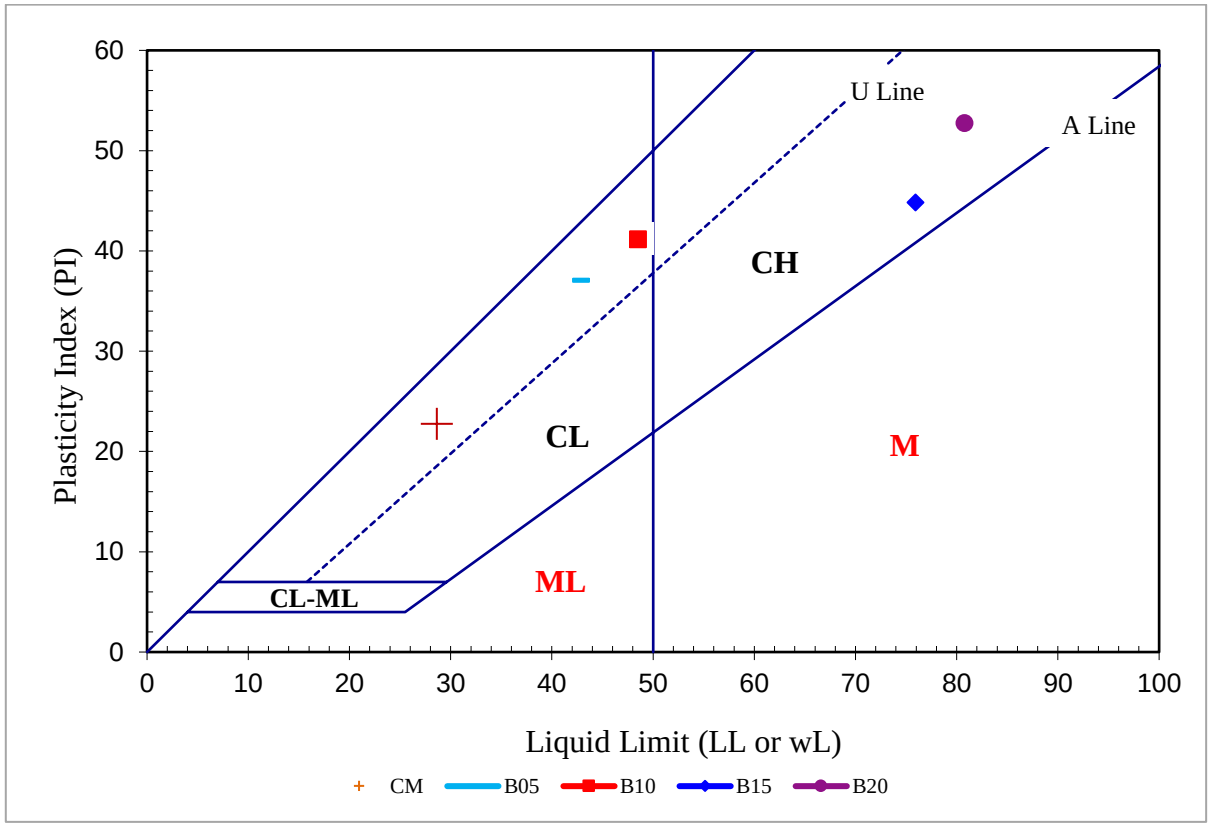


Figure 3-5: Classification of lime-bentonite clay composites based on unified soil classification system

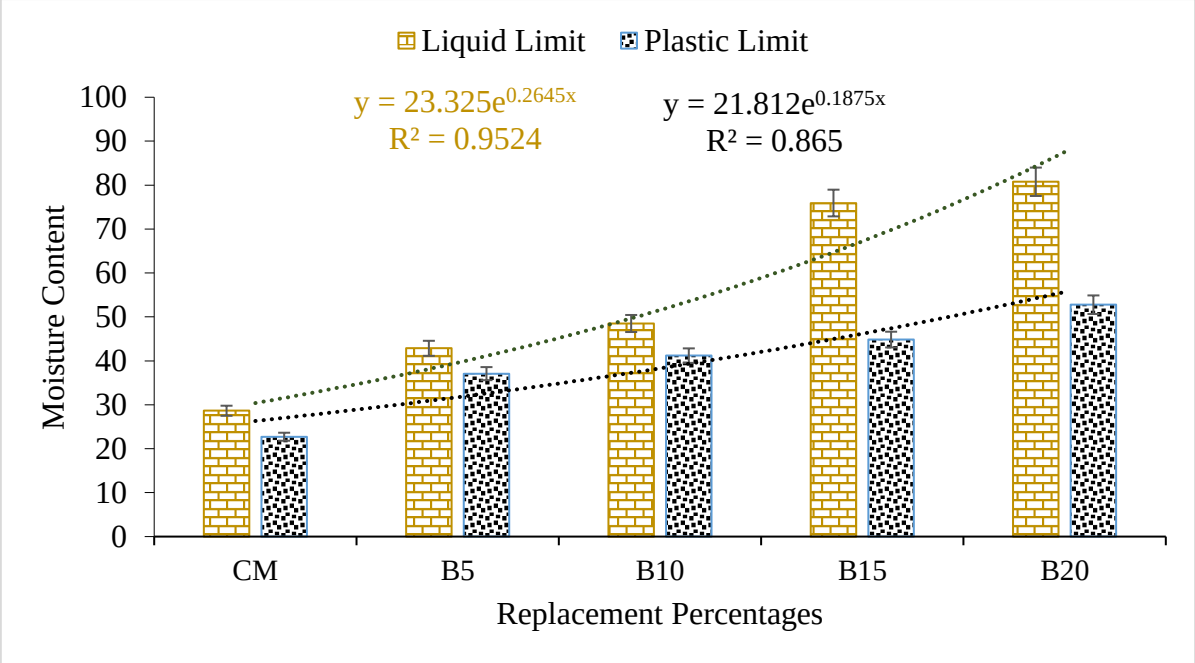


Figure 3-6: Atterberg limits of lime-bentonite clay composites

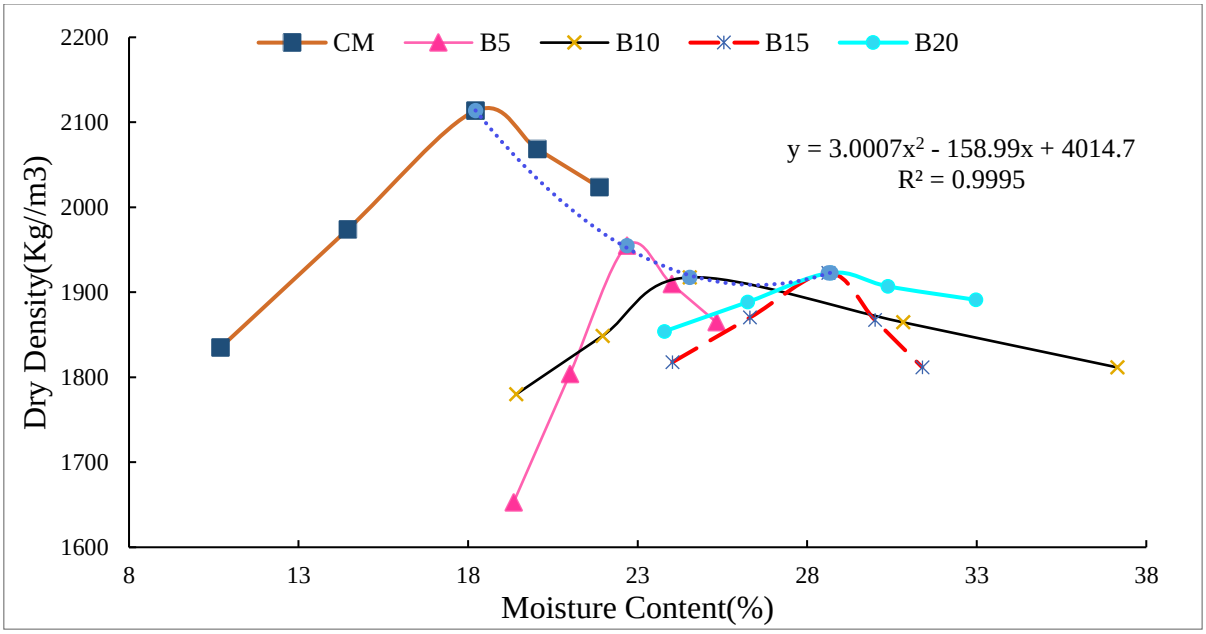


Figure 3-7: Maximum dry density of lime-bentonite clays composites

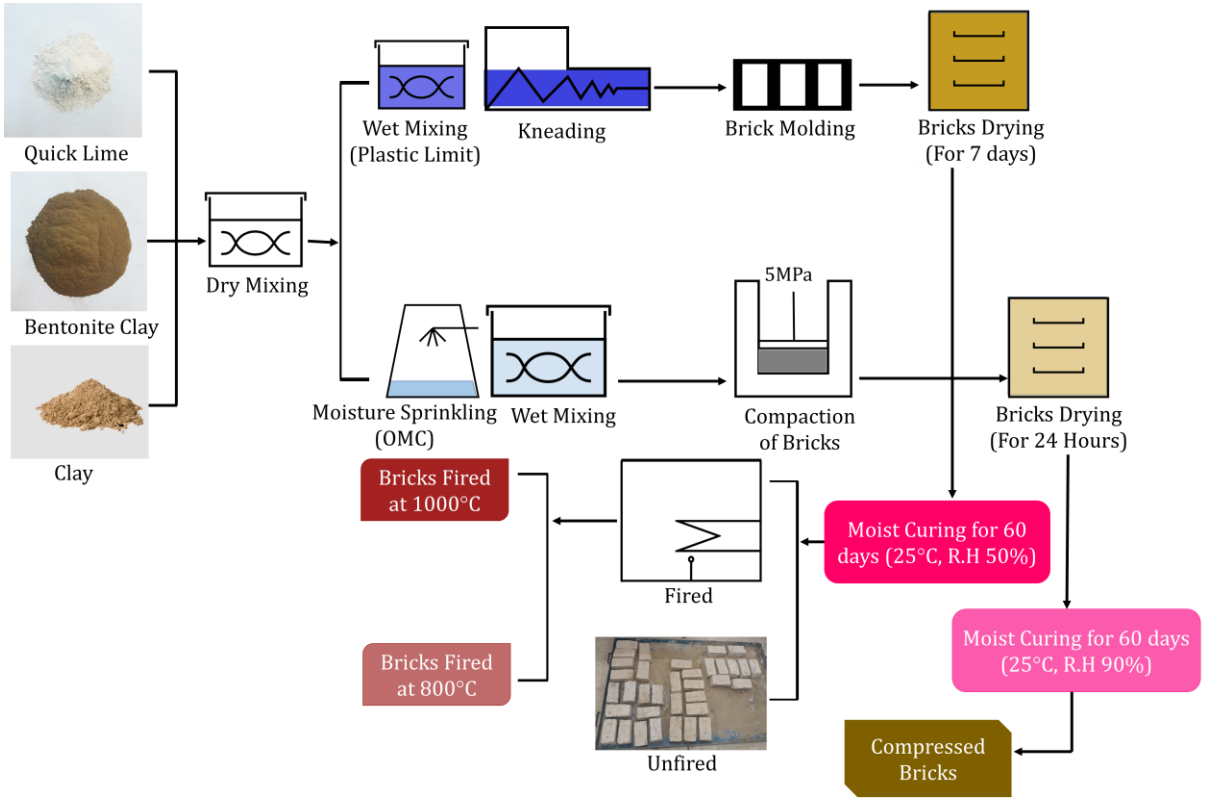


Figure 3-8:Schematics for bricks manufacturing

# Chapter 4

# Discussion of Results

## 4.1. Physical and Mechanical Properties

### 4.1.1. Compressive Strength

Compressive strength is one of the key mechanical property used to add the structural value of the bricks. Based on compressive strength, bricks are classified for various exposure. The values of compressive strength of unfired, compressed bricks, fired at 800 and 1000°C incorporated lime-bentonite clay composite is shown in fig.4-1. Results indicated that the common trend of increased compressive strength with increasing bentonite content was being followed for all types of bricks. Increase in compressive strength observed for compressed, unfired, fired at 1000°C and 800°C bricks from 4.65 to 10.40, 0.83 to 1.38, 1.53 to 3.13, and 1.72 to 2.46 MPa respectively. The regression equations for compressed, unfired, fired at 1000 and 800°C determined as $CS = 3.666e^{0.2019(B.C)}$, $CS = 0.7413e^{0.1342(B.C)}$, $CS = 1.3197e^{0.1748(B.C)}$ and $CS = 1.5414e^{0.0833(B.C)}$ with regression($R^2$) values of 0.98, 0.93, 0.98, and 0.89 respectively. Moreover, compressive strength of certain brick types at various bentonite to lime ratio are shown in fig.4-2. With the increasing B/L the compressive strength increased. The regression equation being shown with the correlation coefficient more than 0.96 translated the good relation between data points and polynomial trend line. However, Compressive strength of lime-bentonite compressed brick satisfied the strength requirement of building code of Pakistan (Building Code of Pakistan 2007) and classified as building bricks for negligible weathering according to ASTM standard C62-13(ASTM, 2013). Applied molding pressure decrease the inter-particle distance and increased the number of interaction points, thus reduced the porosity and increased compressive strength (J.M. Perez, 2014). For unfired bricks, the strength gain observed was due to healing and sealing (Oti, 2010) characterization of sodium bentonite, which expands to fill the available voids attributed to its swelling property. The accelerated consumption of portlandite(formed after hydration of lime) as a result of pozzolanic reaction and formation of calcium silicate hydrate(CSH) and calcium alumino hydrate(CAH) due to dissolution of silica and alumina in saline environment which act as an alkaline to initiate polymerization reaction(Bell, 1996; Glenn, 1963). However, strength gain observed for compressed bricks attributed to reduction of voids, pores by mechanical means and due to pozzolanic reaction between calcium, silica rich lime-bentonite composite. For several agricultural ashes used in unfired clay bricks require alkaline activator to initiate geo-polymerization reaction which occurred between amorphous silica and alumina rich minerals

in the presence of concentrated silicate and hydroxide solution at ambient or elevated temperature constitute stable alumino silicate called geo-polymer. Various researchers used lithium hydroxide, lime/gypsum, sodium hydroxide and sodium silicate as an alkaline activator for initiating geo-polymer reaction. Therefore, Chen et. al. (Chen C, 2012) found lithium hydroxide solution very effective alkaline activator for polymerization reaction in bottom ash incorporated bricks, which resulted compressive strength of bricks up to 28 MPa. Arioz et al.(Arioz O, 2010) studied the fly ash replaced geopolymer clay brick using sodium hydroxide and sodium silicate as an alkali activator. Compressive strength ranged between 5 and 60 MPa with no effect of thermal treatment over strength and density. Freidin (Freidin, 2007) prepared cement less building blocks containing coal fired bottom and fly ash with impregnated polymethyl-hydrogensiloxane (hydrophobic liquid), compressive strength results satisfied the standards. Mohan et. al. (Mohan NV, 2012) investigated the effect of lime/gypsum inclusion in rice husk ash incorporated clay bricks, samples with added lime and gypsum content improved the compressive strength. Ahmari et. al.(Ahmari S, 2012) investigated the copper mine tailing through polymerization reaction, results revealed that samples prepared 15 molar NaOH concentration yielded better compressive strength results than that of 10 molar concentration.

Compressive strength of bricks fired at 1000°C observed were higher than that of 800°C attribute to the optimal sintering temperature of bentonite being achieved around 1000°C. Bentonite particles initiate pore refinement and produce filler effect to densify the microstructure which further get enhanced by sintering due to firing. Various researchers have studied the physico-mechanical properties incorporating agro-industrial waste in clay bricks being fired neared their sintering temperature. Haiying et. al. (Haiying Z, 2011) revealed that the formulation containing 20% of municipal solid waste incinerated ash, 10% feldspar, 10% sand and 60% red ceramic clay has optimal sintering temperature of 950°C with comparatively reduced content of leaching chemicals. Bilgin et. al. (Bilgin N, 2012) showed that the increase mechanical properties of the waste marble dust added fired bricks at 1100°C and up to 10% replacement of granite waste dust does not significantly affected the compressive strength. Quijorna et. al. (Quijorna N, 2012) presented the eco-friendly and resource efficient incorporation of waelz slag in fired clay brick with optimum slag content of 20% by weight of clay. Mezencevova et. al.(Mezencevova A, 2012) used river sediments as sole raw material for brick baking at 1000°C, results revealed that the bricks made by synergic combination of river sediments and clay resulted compressive strength of 29.4MPa which otherwise produced 8.3-11.7 MPa for pure river sediment bricks. Rahman(Rahman, 1987) stated that the incorporation

of rice husk ash yielded the light weight and has comparatively higher strength at firing temperature of 1000°C for 4 hours. Sengupta et. al.(Sengupta P, 2002) revealed that the incorporation of petroleum effluent treatment plant sludge containing hydrocarbons and several metal traces in bricks provide environmental friendly solution with acceptable brick strength as per India Standards, whereas, sintering process restricted the leachate concentration within the allowable limits. Sutcu and Akkurt (Sutcu M, 2009) produced paper processing waste incorporated porous and light weight bricks along reduced thermal conductivity up to 50% than the reference brick without significantly reduction in compressive strength.

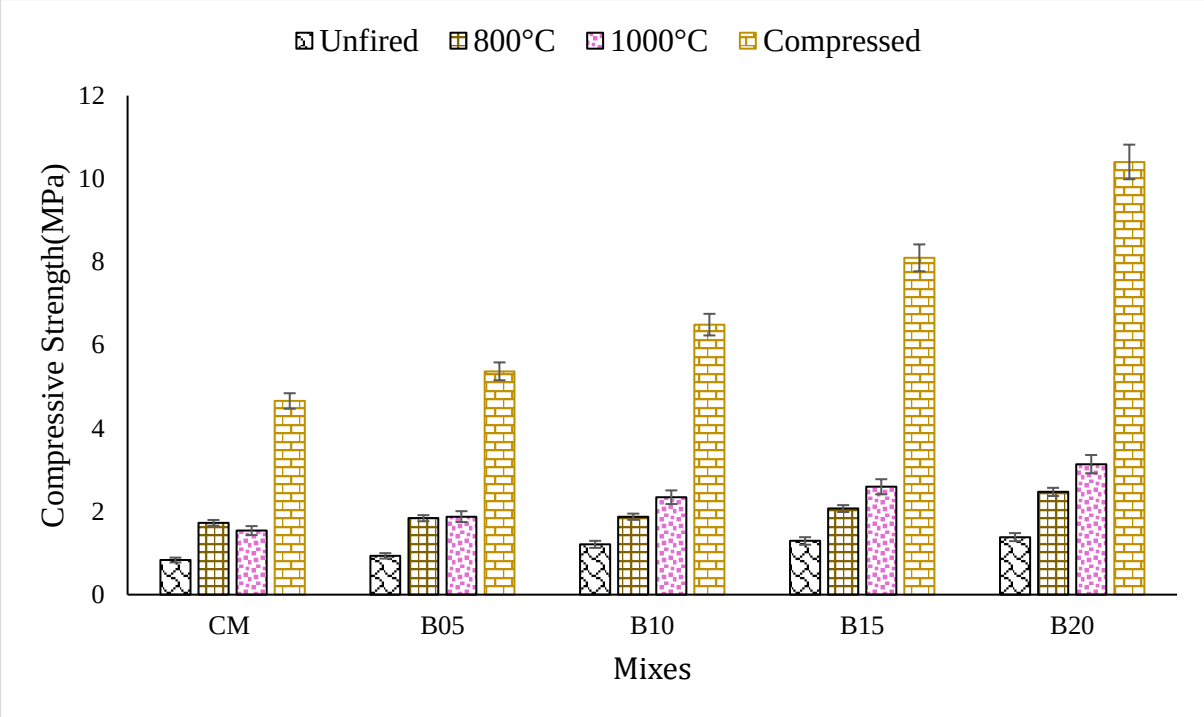


Figure 4-1: Compressive strength of fired and unfired lime-bentonite brick composite at varying concentration of bentonite

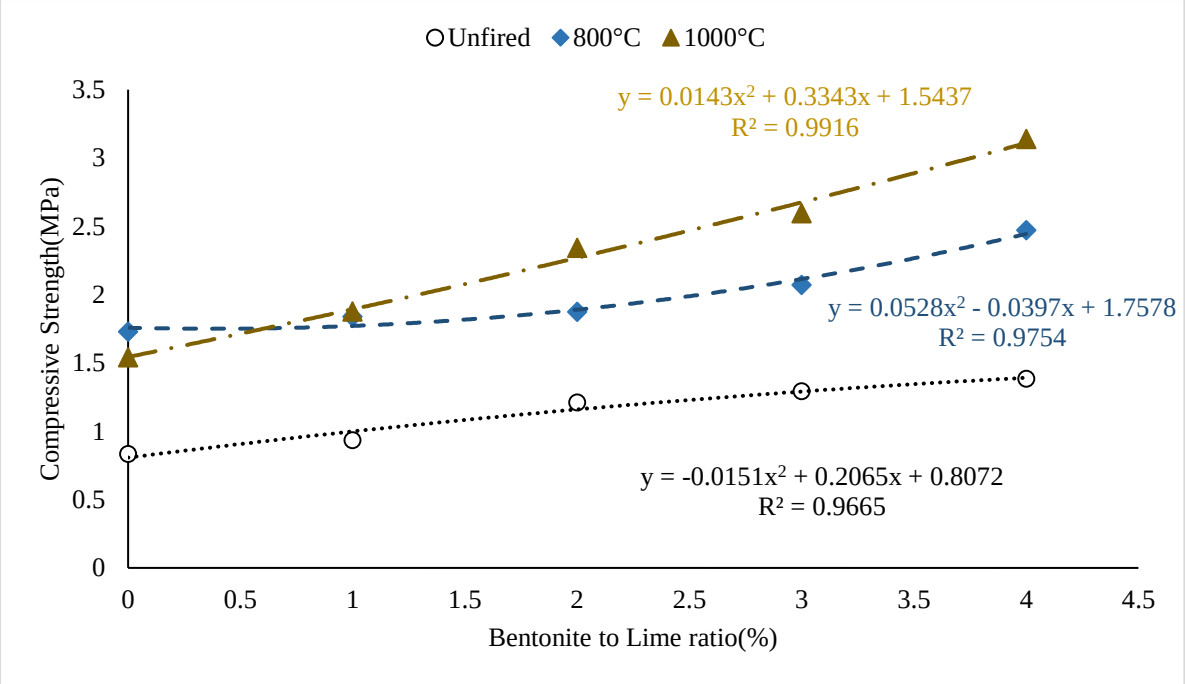


Figure 4-2: Relationship between compressive strength and bentonite to lime ratio of unfired and fired bricks

### 4.1.2. Flexure Strength

Flexure strength of compressed, unfired, fired bricks containing lime-bentonite composite is shown in fig. 4-3. Generally, increasing trend of flexure strength with added bentonite content was observed. Flexure strength of the bricks being compressed, unfired, fired at 1000 and 800°C increased from 0.41 to 1.09, 0.09 to 0.16, 0.16 to 0.30, and 0.18 to 0.29 MPa respectively. The regression equation for compressed, unfired, fired at 1000 and 800°C bricks determined as FS = $0.3208e^{0.2413(B.C)}$, FS = $0.0872e^{0.1342(B.C)}$, FS = $0.1378e^{0.1636(B.C)}$, FS = $0.1639e^{0.1019(B.C)}$ with the correlation coefficients($R^2$) values of 0.99, 0.93, 0.97 and 0.88 respectively. The linear regression relation between compressive strength and flexure strength of the lime-bentonite incorporated bricks as shown in fig. 4-4, which revealed that with the increase of compressive strength values flexure strength also increased. The regression equation for this relation observed as FS = 0.0996(CS) + 0.0151 with correlation coefficient($R^2$) value of 0.99 which indicate the good relation between trend line and distributed data points.

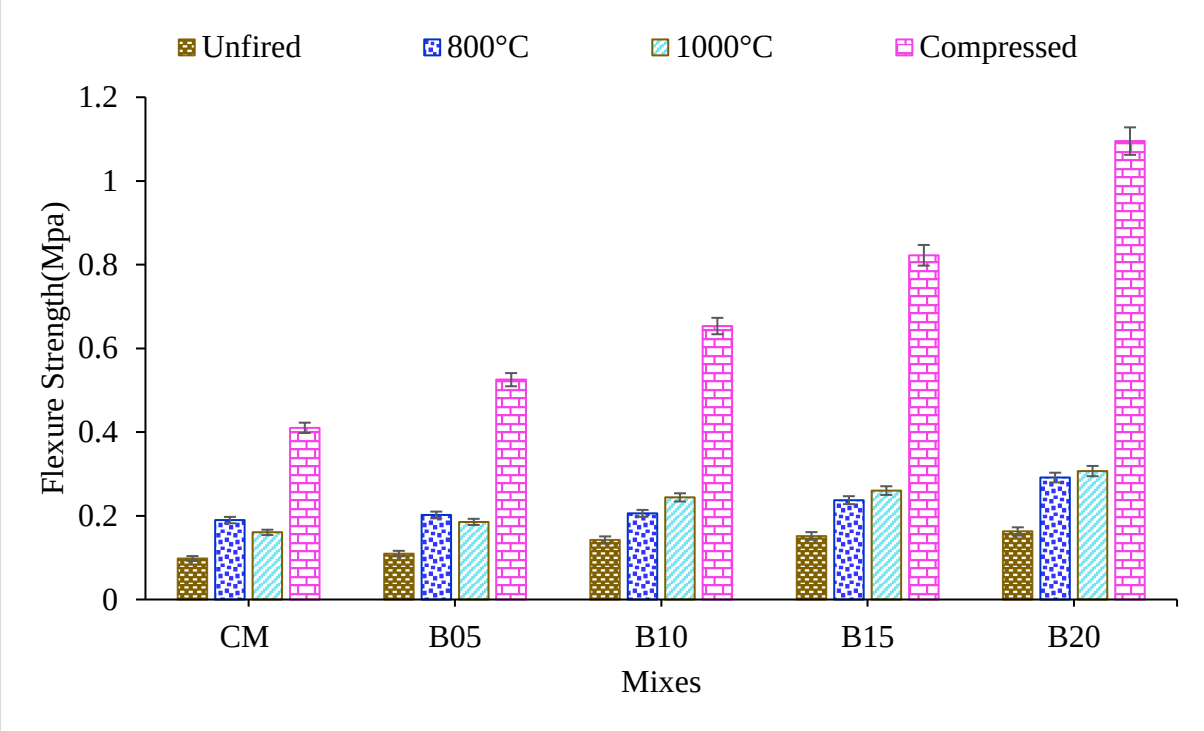


Figure 4-3:Flexure strength of unfired, compressed and fired at 1000°C and 800°C

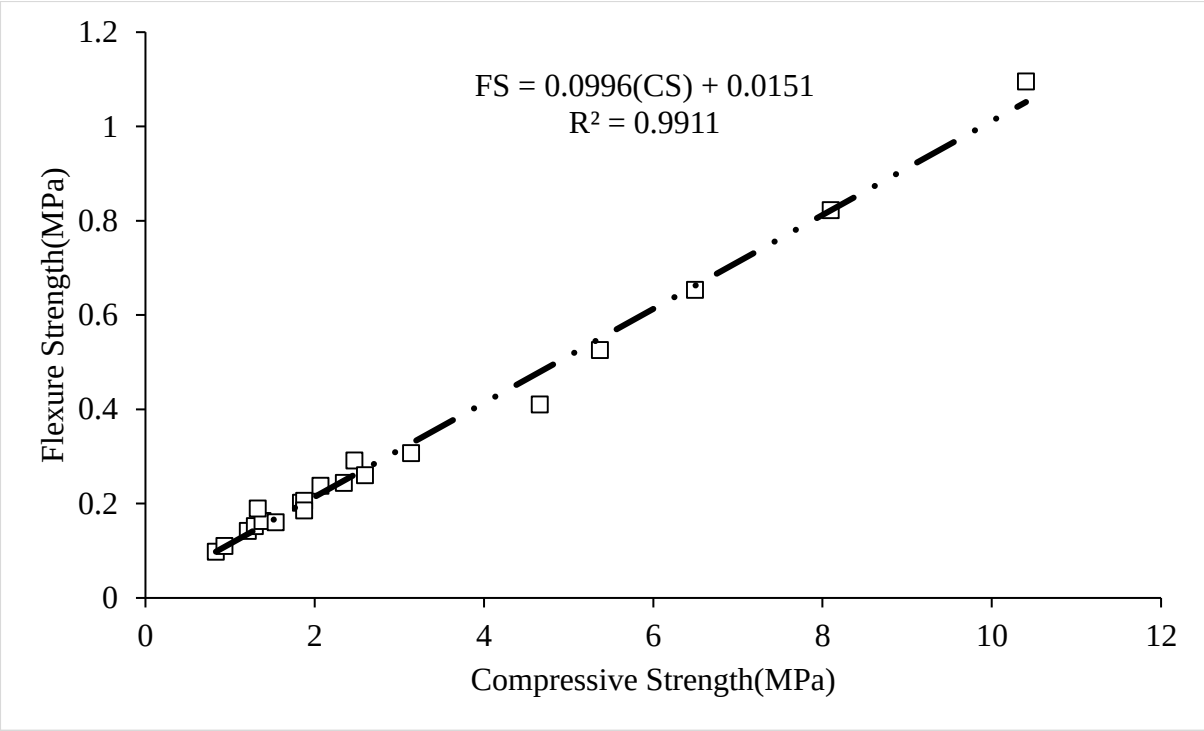


Figure 4-4: Regression relation between compressive and flexure strength of unfired and fired bricks

### 4.1.3. Unit Weight

Unit weight of compressed, unfired and fired at 1000°C and 800°C are shown in fig.4-5. Generally, the unit weight of bricks reduced with incremental values of bentonite replacement. The values of unit weight of compressed bricks was higher due to reduced porosity and inter-

particle voids than unfired and fired bricks. Unit weight of the bricks reduced upon replacement of bentonite content due to expensive nature of bentonite minerals. Sodium montmorillonite absorb water in interlayer region and due to osmotic pressure of water within the bentonite clay minerals cause it to swell (Oti, 2010). The values of unit weight for unfired bricks are higher than that of fired one due to the loss of excessive water being attached physically and chemically bonded within the layers of bentonite as evident from thermogravimetric analysis(fig. 4-11), where the weight loss of B20 composite was highest in the temperature range of dehydration of montmorillonite. Due to this reason unit weight of fired bricks at 1000°C observed was lower as compared to the bricks being fired at 800°C. The reduction in unit weight was observed for compressed and unfired bricks was 5.3 and 14.77% respectively. The exponential regression relation between unit weight and compressive strength being developed is as shown in fig.4-6. Unit weight values lime-bentonite incorporated clay bricks exists within the range of specifications of masonry units (Standards, 2005) and clay masonry units standard (DIN, 2012). Decreasing values of unit weight depicts the increasing content of bentonite, therefore, enhanced pozzolanic activity suspected at higher bentonite content. Hence, compressive strength increased despite of decreasing unit weight values.

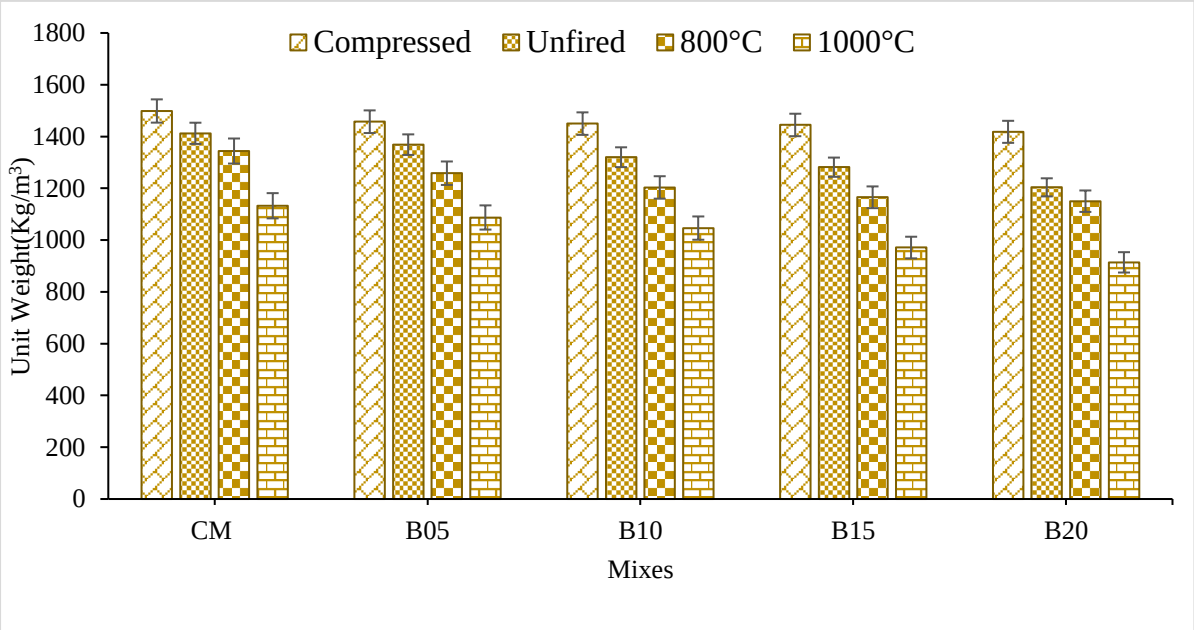


Figure 4-5: Unit Weight of fired and unfired lime-bentonite brick composite at varying concentration of bentonite

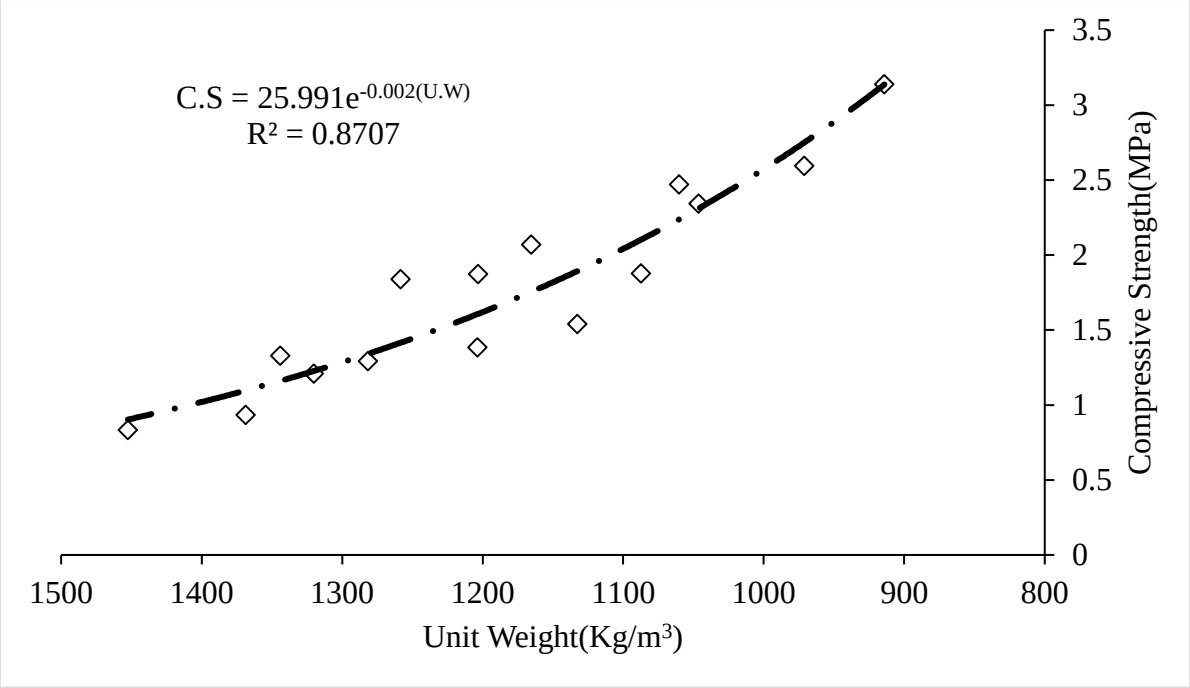


Figure 4-6: Regression relation between unit weight and compressive strength of fired and unfired bricks

### 4.1.4. Water Absorption

Water absorption depicts the amount of permeable pores, voids and capillaries in clay bricks matrix. Water absorption of bricks for unfired, fired and compressed bricks are shown in fig.4-7. Increased incorporation of bentonite in clay bricks reduce the water absorption significantly due to healing and sealing characteristics of bentonite(Francisca Santiago, 2007). Water absorption of compressed, unfired and fired(1000°C & 800°C) bricks reduced from 15.97 to 10.09%, 23.34 to 20.34%, 21.97 to 17.76% and 22.54 to 17.03% respectively. The reduction of water absorption from fired to compressed and from unfired to fired bricks observed was 27.30 and 7.39% respectively. Water absorption of compressed bricks reduced significantly due to the reduced porosity attributed to the applied molding pressure during manufacturing. However, water absorption reduced along the replacement of bentonite in clay brick due to hydration and pozzolanic phases exists within the pores and voids as a chemical interaction between calcium, silica and alumina rich clay minerals in highly saline environment (García-Lodeiro, 2105). Water absorption of unfired bricks is greater than all types due to reduced density of bricks featured to the expensive and swelling nature of bentonite(Francisca Santiago, 2007), as the necessary water was added to achieve the plastic state of the composite during wet mixing of brick constituents, unlike compressed bricks molded samples were not restrained. Hence, no healing/sealing occurred due to swelling of montmorillonite mineral. Fired bricks on the other hand showed the reduced water absorption due to optimal sintering

of the minerals within voids and capillaries, which were being added to the clay brick matrix. Contrary to the all replacement percentage of bentonite, water absorption of CM composite brick was lower at 800°C than at 1000°C due to the optimal sintering of lime occurred at preceding temperature (Han, 2017). Water absorption values of bricks being fired at 1000°C observed were higher than at 800°C due to reduced density of bricks at 1000°C.

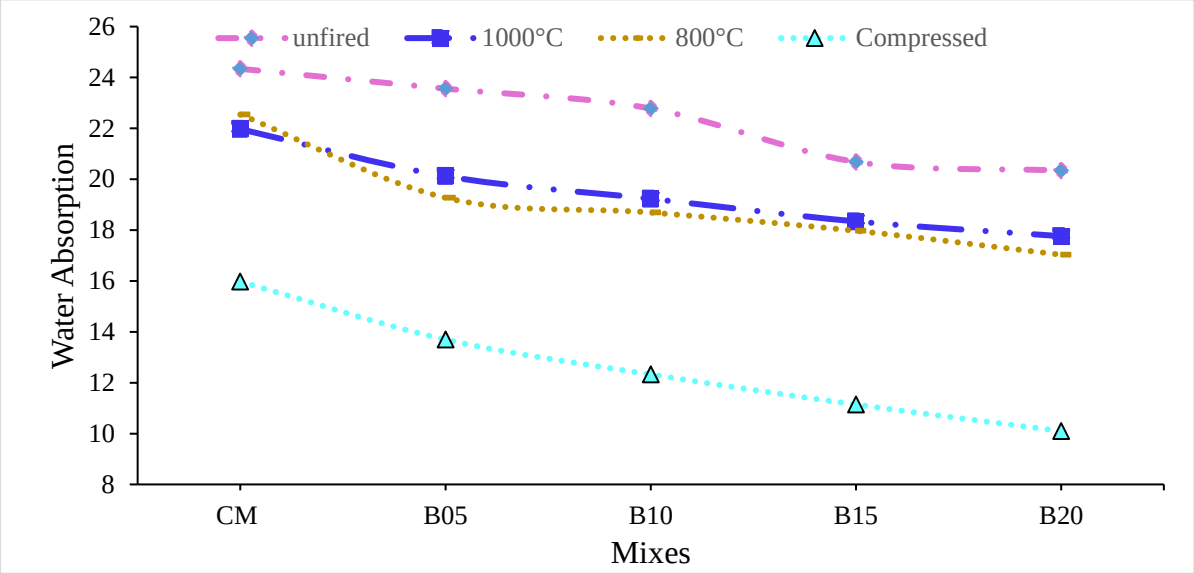


Figure 4-7: Water absorption of lime-bentonite composite incorporated clay compressed, unfired and fired bricks

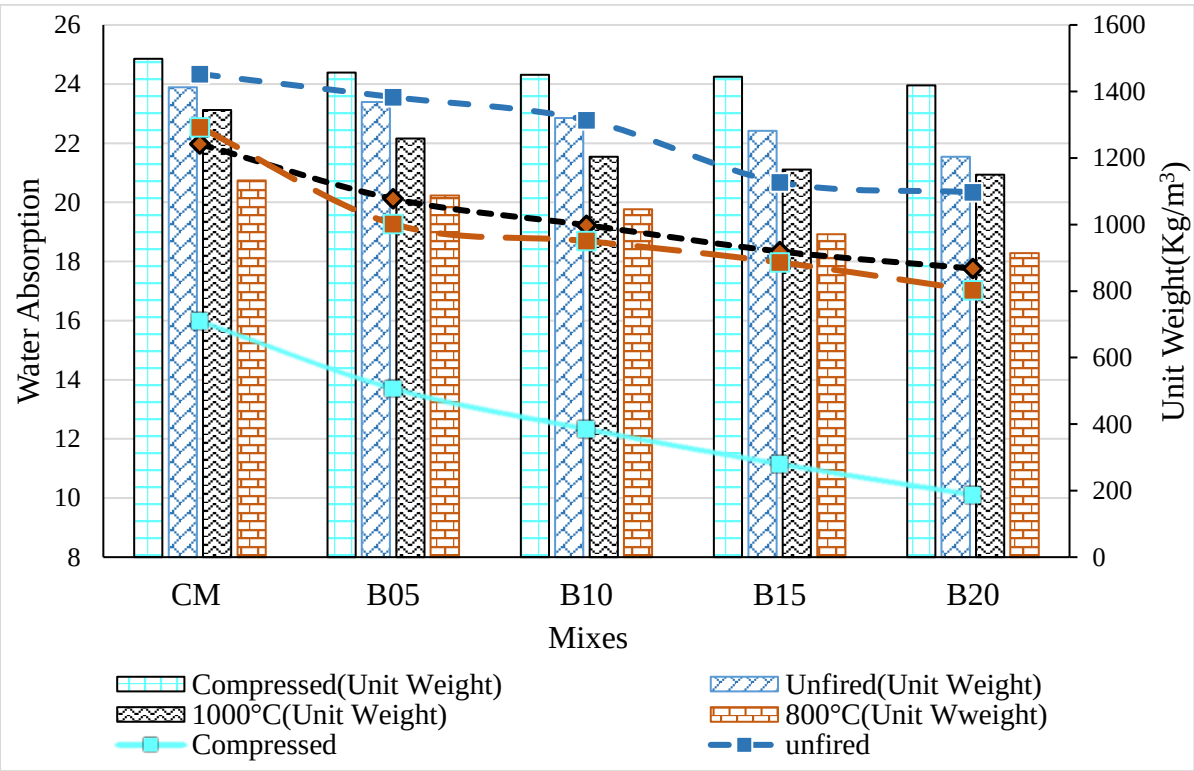


Figure 4-8: Unit weight and water absorption of compressed, unfired and fired bricks

## 4.2. Microstructural Analysis

### 4.2.1. Scanning Electron Microscopy

SEM micrographs along Energy Dispersive Spectroscopy(EDS) of compressed bricks (CM, B10 and B20) containing lime-bentonite clay composite are shown in fig.4-9, whereas, figure 4-10 revealed the SEM micrographs of unfired and fired bricks(800°C and 1000°C). The sequential magnified microstructural morphology of CM, B10 and B20 for compressed brick composites is shown in fig.4-9(a-e), (f-i) and (j-n) respectively. It was interpreted that the addition of varying bentonite content in compressed bricks resulted the densified bright microstructure comprising of calcium silicate hydrate(CSH) and calcium hydroxide(CH) as shown in fig.4-9. Brighter hydration products being generated as a result of hydration of lime bentonite clay composite at higher bentonite replacement level denoted the higher concentration of CSH being evidenced in published literature (Hewlett, 2004; Yazici, 2007). According to Hewlett (2004), calcium silicate hydrate phase might adopt various morphologies such as flakes, fibers, honey combs, tightly packed grains and dense featureless materials at microscopic level, whereas it only exists in foiled morphology at nanometer level.

Therefore, SEM results showed the densification of microstructure occurred both by physical and chemical means i.e. pore refinement by filler effect of micro-nano sized composite particles and synergic pozzolanic reaction of lime-bentonite composite respectively.

However, the concentration of CSH phase identified as flaky and tightly packed grains morphologies increased at highest bentonite replacement being endorsed with calcium to silica(Ca/Si) ratios determined in EDS analysis as shown in Table 3. Ca/Si ratio increased with incorporated bentonite content values of CM, B10 and B20 as 1.09, 1.27 and 1.45 respectively. Increased values of Ca/Si approaches to 1.5 indicated the amorphous nature of hydration products (Hewlett, 2004), which is however clear from the EDS results. SEM micrographs of B20 brick composite(fig.4-9 m) has shown the portlandite formation depicted by the higher calcium content and lower silica content as evident from literature(Hewlett, 2004). The void spaces in lime-bentonite clay matrix ranged between 40-240μm for CM, which were significantly reduced to 10-75 and 2-60 μm for B10 and B20 composites respectively. The reduction in voids by addition of bentonite observed due to the physical filler effect, pozzolanic activity and sealing/healing effect of bentonite endorsed by TGA, XRD and FTIR of the lime-bentonite clay composite which would be discussed later in this section. Free lime and finely grained bentonite particles participated in pozzolanic reaction to generate calcium silicate hydrate (CSH), calcium aluminosilicate hydrate(CASH) and calcium aluminate hydrate (CAH)

in voids to improve the clay matrix (S. B. pally, 2017). Therefore, the microstructure of incremental bentonite added lime stabilized compressed clay brick matrix progressively get enhanced.

SEM micrographs of lime-bentonite added unfired and fired bricks (800°C and 1000°C) is shown in figure 4-10. The magnified microstructural morphology of the CM and B20 brick samples for unfired and fired brick (800°C and 1000°C) are shown in figure 4-10 (a-f), (g-l) and (m-r) respectively. The results of the unfired bricks revealed that the highest concentration of bentonite addition in brick composite produced brighter microstructure(fig.4-10 f), which specifically contain amorphous calcium hydroxide(CH) and calcium silicate hydrate(CSH) attributed to the chemical synergy between lime and bentonite as evident from literature (Hewlett, 2004; Yazici, 2007). Bentonite incorporation densified the microstructure by the formation of higher density bright pozzolanic hydrates in B20 mix(fig 4-10 d, e), whereas comparatively darker lamellar featured particles observed in CM mix(fig 4-10 a, b). The reduction in interspatial voids occurred due to swelling action of bentonite. SEM micrographs of the bricks fired at 800°C indicated the distortion of hydration/pozzolanic phases being characterized by the formation of voids and micro-cracks as shown in fig 4-10 (g-l). The strength gain of the such fired bricks attributed to the clogging of voids and cracks due to pore refinement by the finer particles of lime-bentonite composite and vitrification of lime particles during firing process as sintering temperature of lime is around 800°C being reported in the literature (Borgwardt, 1989). Moreover, the porosity of the fired brick is also governed by the calcium carbonate dissociation between 800-1000°C, as the decomposition of carbonates promotes the formation of voids and fissures evident from literature (Peters T, 1978; Robinson, 1982). Bricks fired at 1000°C undergo densification of microstructure by sintering of bentonite and other clay minerals as shown in fig 4-10 (m-r), in which cracks, voids and fissures were clogged and grains get connected with each other by coalescence of the particles. Hence, for unfired bricks the densification of microstructure occurred due to pore refinement by filler effect as well as pozzolanic activity/geo-polymerization reaction, whereas for fired bricks the lamellar featured microstructural particles of clay bricks get densified by the sintering of minerals associated with lime-bentonite composite, thus increased the mechanical properties of clay bricks at corresponding sintering temperature of the incorporated minerals.

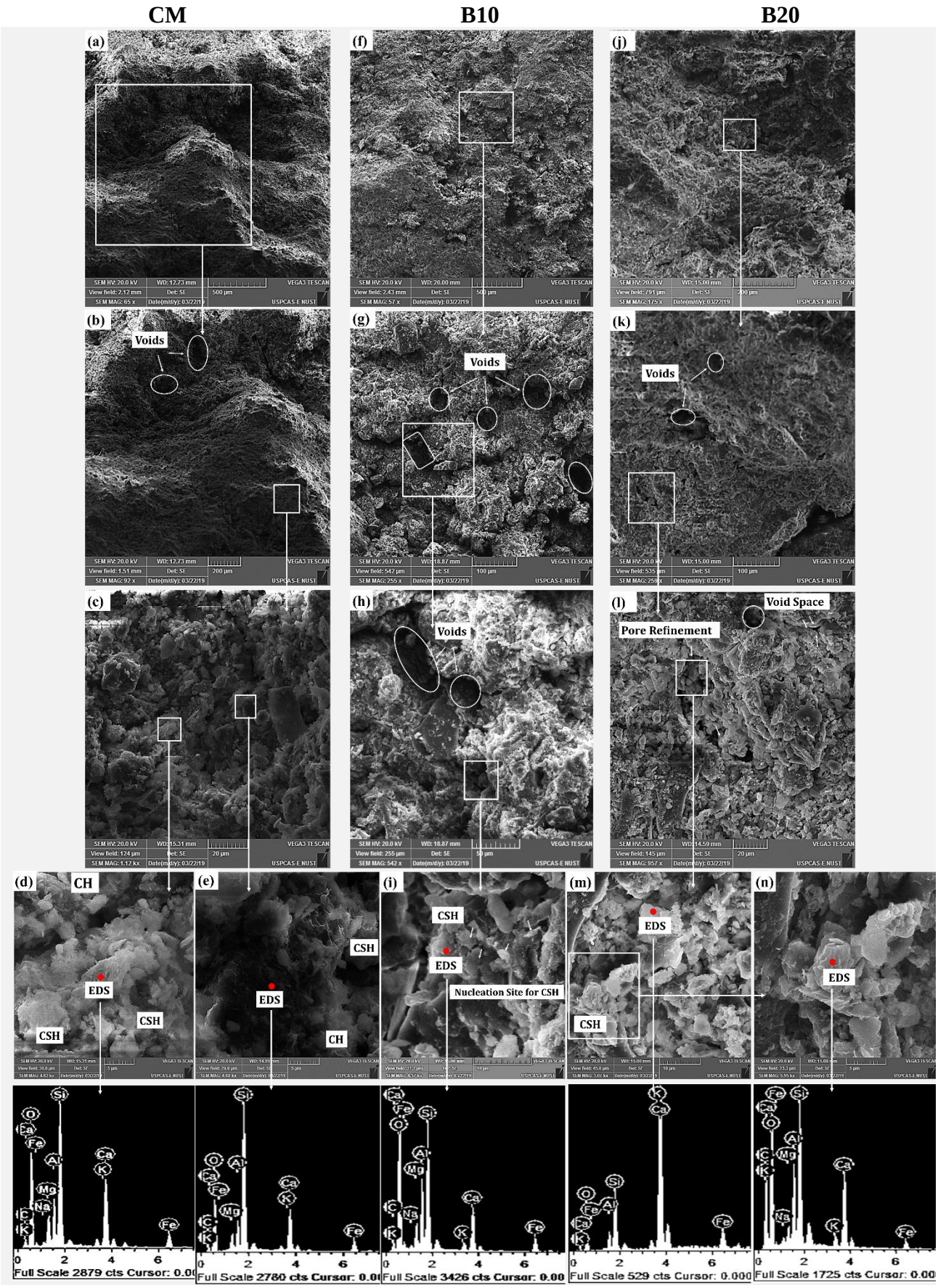


Figure 4-9: Scanning Electron Microscopy(SEM) and Energy Dispersive Spectroscopy(EDS) of compressed bricks composites

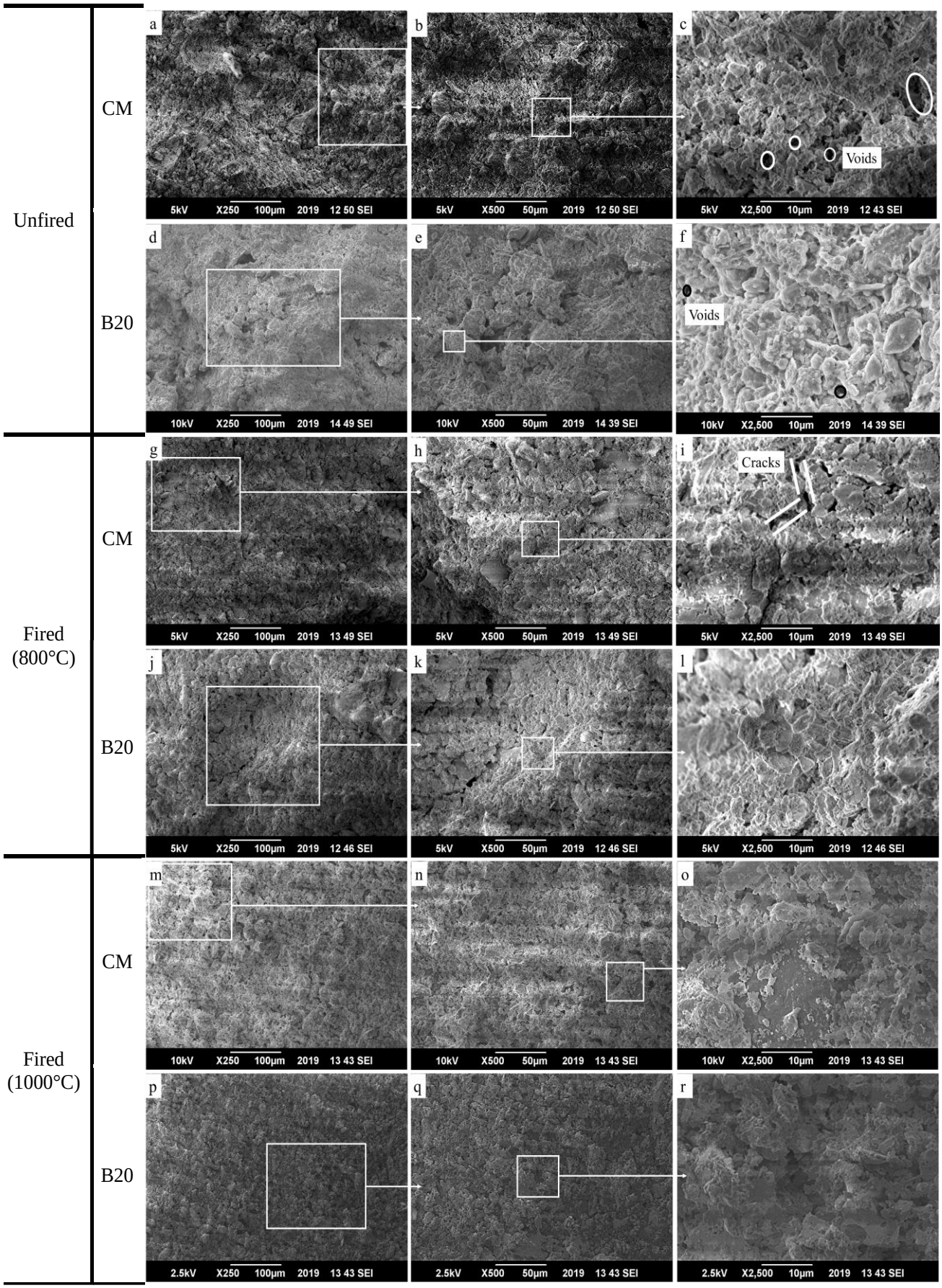


Figure 4-10: SEM micrographs of lime-bentonite incorporated unfired, fired bricks (800°C, 1000°C)

Table 4-1: Ca/Si and Ca/(Si+Al) of compressed bricks

| Elements | Percentage Atomic Weight | | |
|---|---|---|---|
| | CM | B10 | B20 |
| Ca/Si ratio | 1.09 | 1.27 | 1.45 |
| Ca/(Si+Al) | 1.21 | 0.92 | 0.89 |

### 4.2.2. Thermogravimetric Analysis

Thermogravimetric analysis of lime bentonite clay composite as shown in fig. 4-11 revealed the several weight loss regions. First weight loss region attributed to the dehydration of clay minerals up to 150°C, in which physically adsorbed water on the surface and chemically bonded water within the layers dissociated. Decomposition of hydration phases occurred between temperature range of 150-390°C, in which water present in CSH gel evaporated and decomposition of CSH hydration phase occurred, whereas, between the range of 390-460°C dehydroxylation of portlandite occurred due to release of hydroxyl group in this temperature range. Dehydroxylation of montmorillonite occurred between 460-700°C. Weight loss of lime bentonite compressed clay brick composite summarized in Table 4-2, which was tested at curing age of 90 days. In order to investigate the qualitative nature of hydration and pozzolanic products, comparison for weight loss of composite sample within the temperature ranges linked with calcium silicate hydrate and portlandite can justify the evident of pozzolanic activity from literature(S. A. Memon, 2019). Temperature range between 150-390°C corresponds to the dissociation of calcium silicate hydrate, whereas 390-460°C associated with the dehydroxylation of portlandite. The weight loss in temperature region linked with CSH has highest values of 3.35% for B20 mix and minimum values of 3.04% for CM composite attributed to enhanced microstructure due to lime-bentonite synergic hydration occurred in bentonite rich composite, which is evident from bright regions revealed in SEM analysis(fig. 4-11 m). Least weight loss of 0.75% observed in the temperature region associated with dehydroxylation of portlandite observed for B20 formulation and maximum values of 2.25 for CM formulation attributed to the pozzolanic reaction, in which portlandite get consumed resulting the CSH gel in B20 formulation due to higher surface area and high ion exchange capability of montmorillonite present in bentonite (Boardman, 2001; E. Vitale 2017). However, B10 formulation exists between CM and B20 in terms of weight loss of portlandite and CSH gel. Therefore, thermogravimetric analysis of lime bentonite composite endorsed the results above analyzed microstructural and physico-mechanical results.

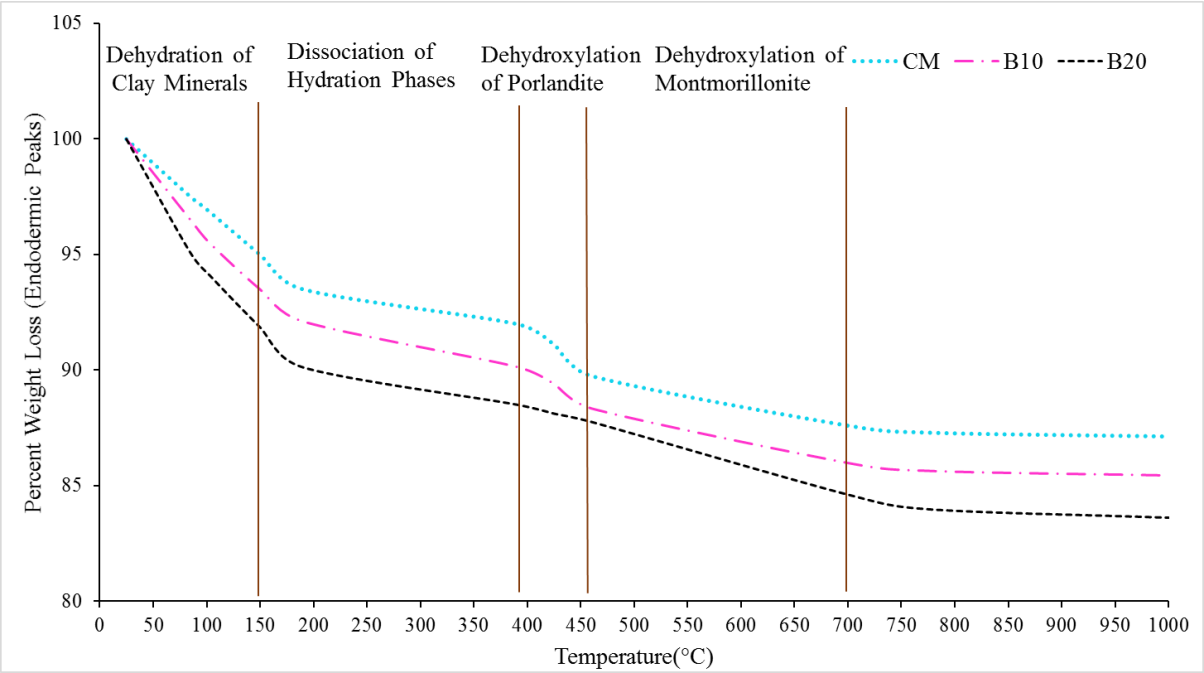


Figure 4-11: Thermogravimetric analysis of lime-bentonite added compressed clay bricks

Table 4-2: Thermogravimetric analysis of the lime-bentonite incorporated compressed bricks

| Mixes | Percent weight loss at various temperature ranges | | | |
|---|---|---|---|---|
| | Temperature Ranges | | | |
| | Up to 150°C | 150-390°C | 390-460°C | 460-700°C |
| CM | 5.02 | 3.04 | 2.25 | 2.15 |
| B10 | 6.5 | 3.15 | 2.01 | 2.36 |
| B20 | 8.15 | 3.35 | 0.75 | 3.15 |

### 4.2.3. X-Ray Diffraction

X-ray diffraction of the samples taken from compressed, unfired and fired(800°C, 1000°C) lime-bentonite incorporated clay bricks was conducted to identify the hydration products based on their crystallographic nature and draw the qualitative intensity comparison of hydration products among bentonite replacement levels. Phase diffraction peaks were identified for all brick types mentioned at various 2θ diffraction angles as shown in fig.4-12 and 4-13. Phase diffraction angles being identified for peaks of CSH, Albite and Calcite were 28.09(3.17Å), 27.82(3.20 Å), and 29.41(3.03 Å) respectively, whereas quartz and portlandite were identified at 20.76 (4.27Å), 26.68(3.34Å), 39.47(2.28Å) and 36.88(2.43Å), 50.30(1.81Å) respectively as a result of pozzolanic reaction between silica and lime rich minerals in saline environment. Phase diffraction peaks for B20 mix of bricks fired at 800°C resulted the intensified peaks of quartz and calcite due to sintering of minerals at mentioned temperature, whereas, at firing temperature of 1000°C the reduced crystallinity of the quartz and calcite indicated by the lower

intensity from CM to B20 mix. Contrarily, the intensity of peak for unfired brick get reduced from CM to B20 mix due to formation of amorphous hydration phases. Moreover, highly concentrated quartz in CM mix reacted with portlandite to form calcium silicate hydrates marked by lower intensity peaks due to their amorphous nature.

Similar to the unfired brick samples, XRD plot of compressed brick samples is shown in fig. 4-12, which indicated the phase diffraction peaks of quartz, albite, calcite and calcium silicate hydrate observed were intensified. Due to alkaline nature of lime-bentonite clay composite, clay brick matrix underwent pozzolanic reaction at faster pace between portlandite (formed during hydration of lime) and siliceous/aluminous bentonite minerals to produce calcium silicate hydrate gel, therefore, lower intensity of portlandite (CH) were observed in XRD plot of B20 compressed clay brick. According to Glenn (1963), lime-clay mineral interaction in the presence of water caused the hydration of quick lime which evolve high concentration of calcium ions, generate portlandite, increase the pH of clay matrix and facilitate ion exchange between calcium ions and clay cations resulted the dissolution of silica and aluminum which reacted with calcium ions to produce calcium silicate hydrate(CSH), therefore, current study observed similar products as evident from XRD results. Moreover, E. Vitale et. al. (E. Vitale 2017) conducted the multiscale analysis of lime treated bentonite, their crystallographic phase diffraction results are similar to that of compressed bricks, in which bentonite inclusion cause reduction of portlandite due to its consumption by pozzolanic reaction.

X-ray diffraction results of unfired and fired bricks for CM and B20 mix shown in fig. 4-13. The chemical reaction between silica/alumina rich minerals and portlandite produced calcium silicate hydrate as a result of pozzolanic reaction. Therefore, reduced intensity of peaks observed for unfired bricks attributed to the dissolution of minerals to produce amorphous phases. For bricks fired at 800°C, high intensity peaks of quartz and calcite was observed due to crystallization of the mentioned minerals as a result of sintering temperature being reached. The X-ray diffraction results of bricks fired at 1000°C revealed the reduced peaks of quartz, calcite and CSH comparative to that of 800°C firing temperature, because at higher firing temperature the crystalline structure of the minerals distort. At 1000°C, complete dissociation of calcite, albite and CSH was observed for CM mix, which otherwise progressively dissociated for B20 mix attributed to higher stability of bentonite rich mix. Hence, densified brick microstructure was achieved by pozzolanic reaction for B20 mix of unfired brick, whereas, optimal sintering of included minerals composite for B20 mix of fired brick samples.

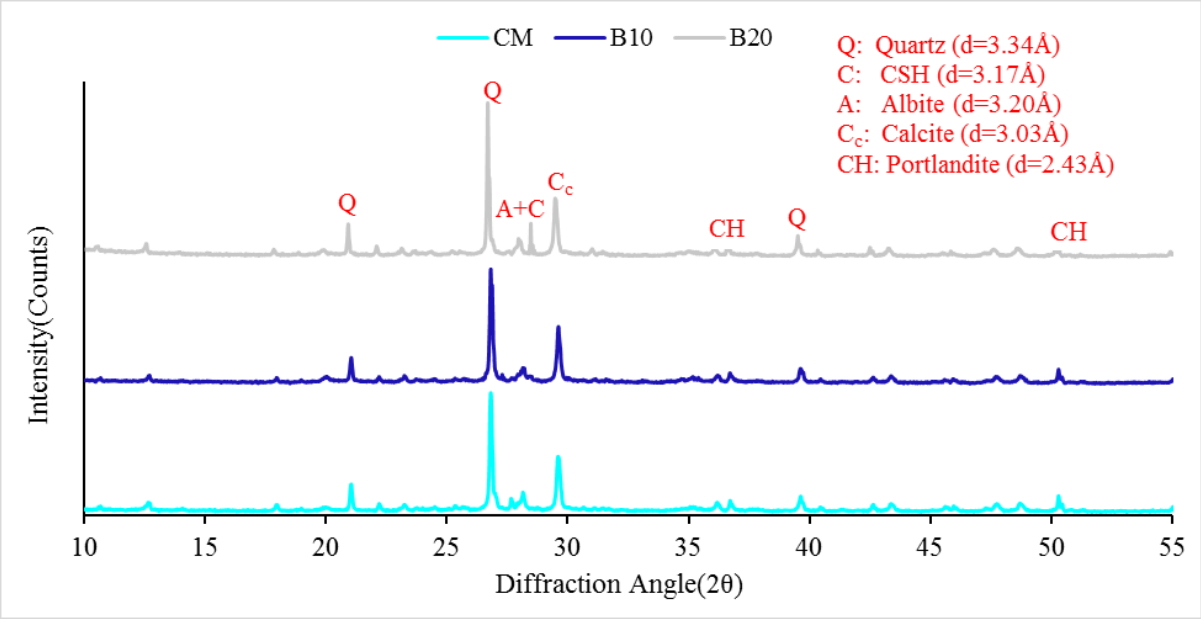


Figure 4-12: X-ray diffraction(CuK radiation) of compressed lime-bentonite clay bricks at 90 days curing age

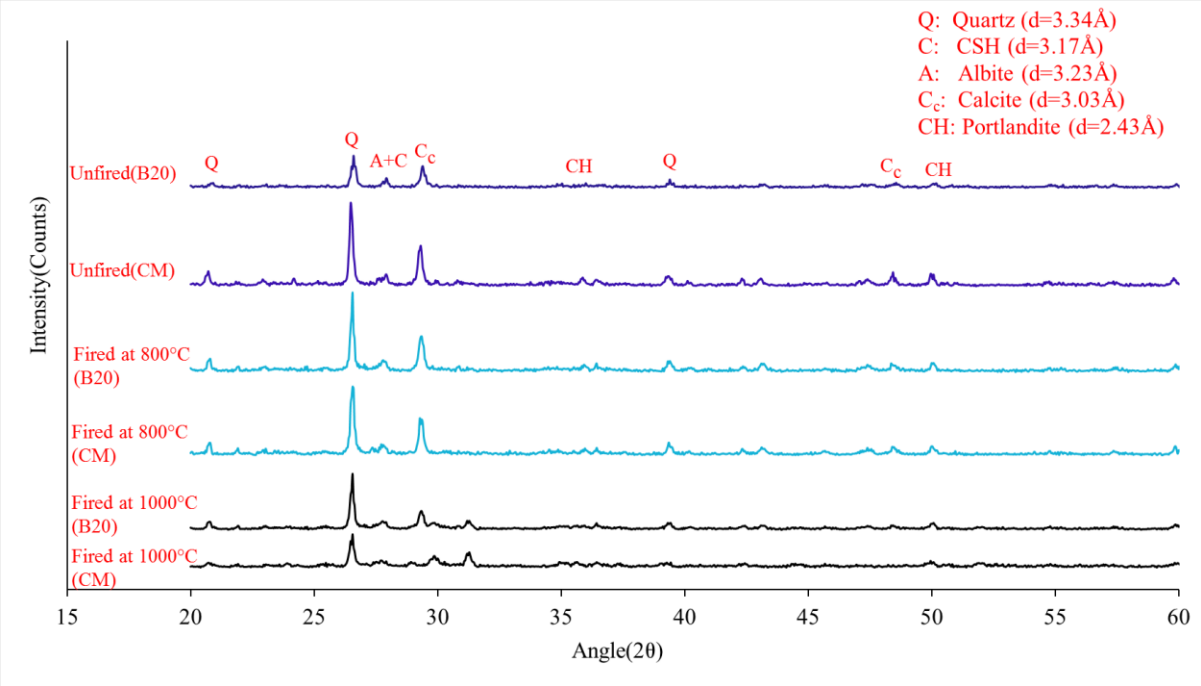


Figure 4-13:X-ray diffraction (Cu-K radiation) of unfired and fired brick(800°C and 1000°C)

### 4.2.1. Fourier Transform Infrared Spectroscopy

Fourier transform infrared spectra of the powdered samples taken from CM and B20 mixes for compressed, unfired and fired(800°C, 1000°C) brick types containing lime-bentonite composite at varying bentonite content is shown in fig. 4-14. FTIR plot identify the hydration phases based on intensity of absorbed infrared energy frequency bands by chemical bonds of the hydration phases at their natural frequency. According to D. Eliche-Quesadaa (2018), the frequency bands are classified into three broad bond vibration frequency ranges, which are

850-1200, 1200-1800 and 3000-3800 cm-1. The first frequency band(850-1200 cm-1) is associated with the stretching vibration of water molecule present in CSH gel formed as a results of clay hydration as evident from literature (D. Eliche-Quesadaa, 2018),the stretching vibrational modes of Si-O broad absorption peaks observed at 871.82 and 983.69 cm-1. Moreover, the presence of amorphous silica was found approximately at 1000 cm-1. Sharp intense peak of Si-O was observed at 871.82 cm-1 for compressed and unfired bricks, whereas, for unfired bricks the peak intensity of B20 mix was higher due to excessive hydration (peak 3, peak 1) attributed to bentonite inclusion. However, peak(2,3) reduced for brick fired at 800°C and ultimately get broadened at 1000°C firing temperature attributed to dissociation and recrystallization of mineral phases due to their sintering.

The aluminate frequency bands were appeared at 569 cm-1 (F. Allali, 2016) due to progressive inclusion of bentonite clay in the mixes; whereas, second region is assigned to the C-O bond stretching and bending vibration of aragonite was observed at 1408 cm-1 peak(D. Eliche-Quesadaa, 2018). Highest shoulder peak was observed at 569 cm-1 for higher concentration of aluminate phase in unfired B20 mix due to higher extent of geo-polymerization occurred attributed to the higher dilution of alkaline activator(Ca(OH)2) because of highest mixed water content(plastic limit). Broader peak associated with the C-O bond bending vibration of aragonite reduced at 800°C and finally disappeared at 1000°C firing temperature due to decomposition of calcium carbonate. In the third absorption region, the prominent peak observed at 3620 cm-1 which attributed to the stretching vibration of hydroxyl group in portlandite. The peaks(2,3) associated with CSH gel get broaden and intensified due to formation pozzolanic hydrates. Calcium aluminate hydrate peaks(1) became prominent at higher replacements of bentonite attributed to the dissolution of silica and alumina rich minerals due to higher ion exchange capability of bentonite(Ca2+) in the presence of concentrated Ca(OH)2, which yielded higher concentrations of calcium aluminate hydrate as depicted in enhancement of microstructure in SEM analysis. FTIR results of unfired brick samples are similar to Kae-Long Lin (2014) and Kang Gao (2014), in which waste catalyst cement paste and nano silica metakaolin based geopolymer respectively was analyzed for investigating their properties. The strength results of waste catalyst cement paste and nano-silica nano silica based geopolymer enhanced by densification of microstructure attributed to pozzolanic activity and geo-polymerization reaction. Therefore, compositional analysis of compressed and unfired bricks revealed the evidence of pozzolanic activity and geo-polymerization reaction, whereas, fired brick showed that vitrification of minerals occurred at their optimum sintering temperature(1000°C).

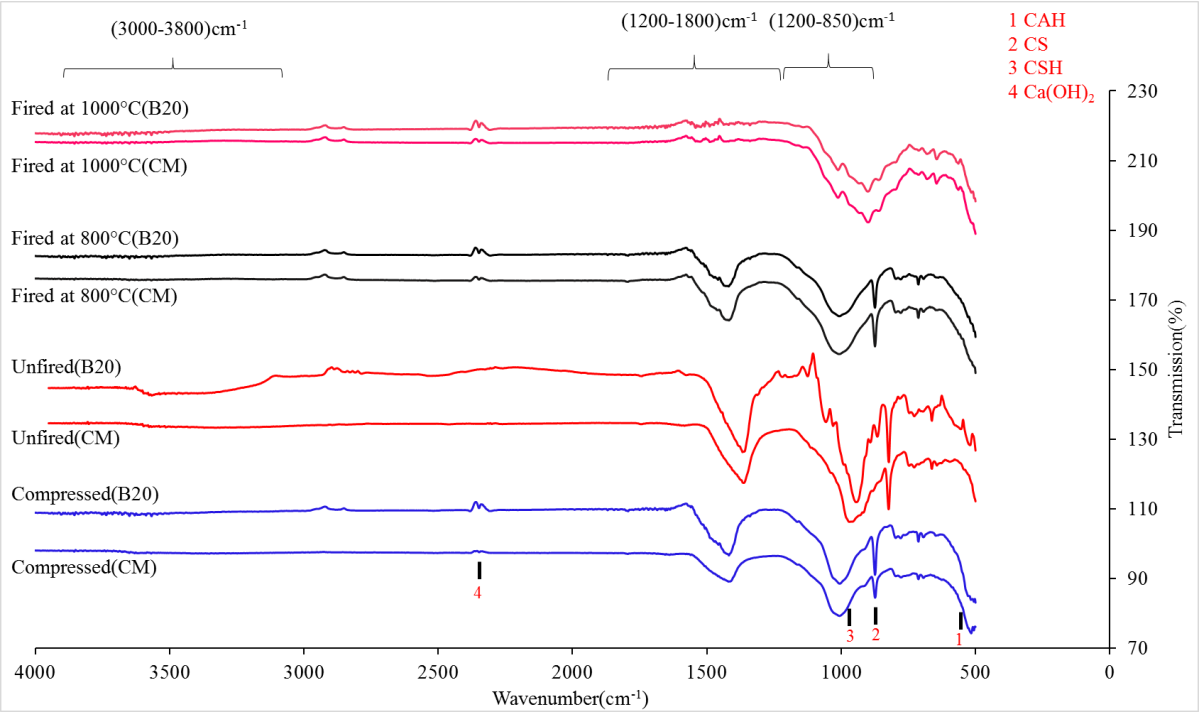


Figure 4-14: Fourier Transform Infrared Spectroscopy spectra of unfired bricks containing lime-bentonite composite

## 4.3. Thermal Properties

Thermal conductivity values of compressed clay bricks at varying bentonite replacement percentages as shown in fig. 4-15 revealed that thermal conductivity of bricks decreased with the increased bentonite content attributed to expensive/swelling cause due to osmotic pressure generated by the bentonite's interlayer absorbed water. Thermal conductivity of compacted bentonite composite depends on dry density, the water content, and mineralogical composition (De Vries, 1963; Johansen, 1975). Dry density and water content is directly related to the thermal conductivity of lime-bentonite incorporated compressed clay bricks. However, the results have shown that the decreased dry density with incremental bentonite content and therefore, is the thermal conductivity. Maximum reduction in thermal conductivity at highest replacement of bentonite observed was 47.22%, comparative to conventional fired brick(CFB), whereas the reduction for CM, B05, B10 and B15 was 29.16, 34.72, 40.27, 44.44 and 47.22 % respectively. It is also evident in the literature(Hayati-Ashtiani, 2013) that the micro and nano sized pore exists within the bentonite microstructure which may contribute toward the reduced thermal conductivity. Moreover, regression relation between unit weight and thermal conductivity is shown in fig. 4-17 indicating both properties are directly proportional with correlation coefficient value of 0.96 indicating good relation between data points and exponential trend line. Thermal conductivity values of compressed bricks ranged between 0.38-0.51 W/m-K which is in line with literature (Wisal Ahmed, 2018 ). However, reduction in

thermal conductivity of in comparison with conventional fired bricks(CFB) is significant, therefore it can be classified as thermal insulated building bricks for structural use.

Table 4-3:Thermal conductivity, total heat gain, cooling load reduction and CO2 emission for compressed bricks

| Mix Designation | Thermal Conductivity | Total Heat gain | | Cooling Load Reduction | $CO_2$ Emissions |
|---|---|---|---|---|---|
| | w/m-K | (BTUs) | (TR) | % | (Per annum(Kg)) |
| CFB(reference) | 0.72 | 12785.17 | 1.07 | - | 971.28 |
| CM | 0.51 | 10295.01 | 0.86 | 19.48 | 782.11 |
| B05 | 0.47 | 9798.27 | 0.82 | 23.36 | 744.37 |
| B10 | 0.43 | 9301.54 | 0.77 | 27.25 | 706.63 |
| B15 | 0.40 | 9003.19 | 0.75 | 29.58 | 683.97 |
| B20 | 0.38 | 8704.83 | 0.73 | 31.91 | 661.30 |

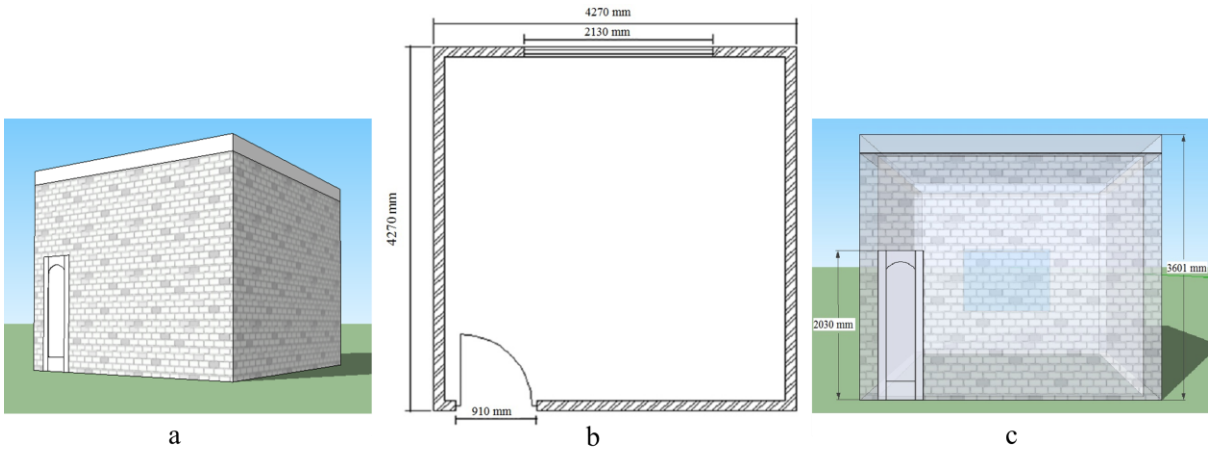


Figure 4-15: a) Prospective view, b) Plan c) Elevation of prototype room being drafted in Google sketchup and Autocad

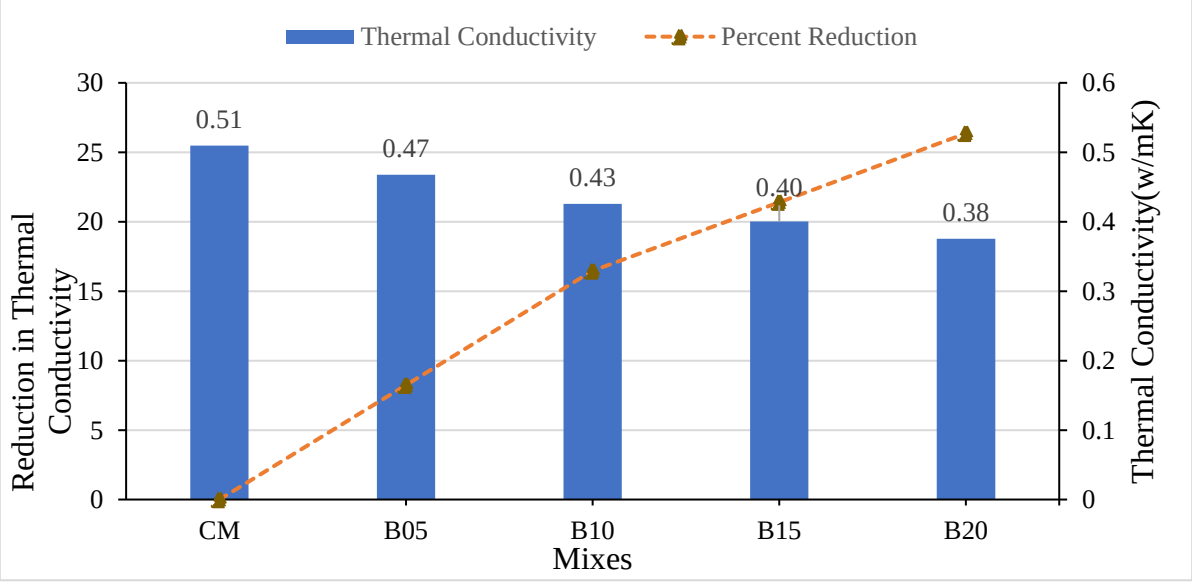


Figure 4-16: Thermal Conductivity and percentage reduction in thermal conductivity

### 4.3.1. Energy Efficiency And Carbon Emissions

Incremental replacement of bentonite in lime stabilized clay brick resulted lower density and thermal conductivity, which imparts sustainability and cause energy conservation by reducing the energy consumed heat ventilation and air conditioning (HVAC) system in building. Energy conservation of the building containing lime bentonite compressed clay bricks walls was investigated for its energy efficiency using a single prototype room with all sides being exposed to climate conditions having dimensions (4270 mm x4270 mm x 3601 mm) as shown in fig. 4-15. Thicknesses of roof and wall were taken as 254 and 229 mm respectively. The net heat gain of the components (walls & roof) was determine in refrigeration ton(TR) and British thermal units(BTU) from standard equations. In prototype room, door and window were installed at its front and rear with corresponding thermal coefficient values taken to determine net heat gain. Net cooling load reduction determined for the prototype room was calculated as shown in Table 5, resulted the heat reduction values of 19.48, 23.36, 27.25, 29.58 and 31.91% for CM, B05, B10, B15 and B20 composites respectively.

For presenting its eco-friendly aspect, reduction of carbon emission for lime-bentonite added compressed bricks can be estimated for heat extraction capacity of heat ventilation and air conditioning(HVAC) system. Published literature(Kumar, 2013) revealed that the carbon footprints for 1.5 ton air conditioner are 1368 kg per annum on average, if it operates 8 hours a day and 20 days per months. Total annual carbon footprints can be estimated based on above assumptions for all lime-bentonite compressed clay bricks as shown in Table 5. The maximum of 15.44% reduction in carbon emission yielded for B20. Therefore, lime-bentonite compressed clay bricks produced favorable results for thermally insulated building bricks, which provides indigenous, energy efficient, eco-friendly and sustainable options against conventionally fired bricks.

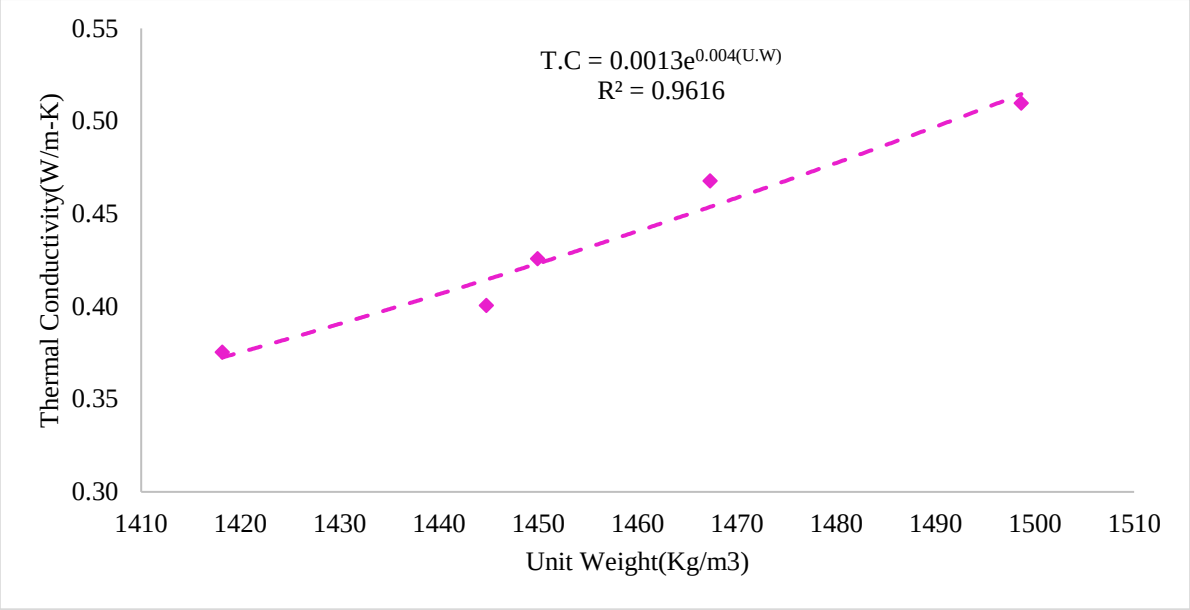


Figure 4-17:Relation between unit weight and thermal conductivity

### 4.4. Sulphate Resistance

Acid attack results in the form of corrosion resistance($\sigma_a/\sigma_n$) and weight gain is shown in fig. 4-18. The corrosion resistance and percentage weight loss values of the compressed brick increased with the incremental bentonite content ranged between 0.72 to 0.81 and 22.28 to 4.27% respectively. Highest corrosion resistance value for sulphuric acid at B20 composite was observed attributed to the consumption of leachable portlandite content($Ca(OH)_2$) to form denser secondary CSH and CASH during the pozzolanic reaction between silica, alumina rich bentonite and portlandite (Alaa Shakir, 2015), whereas, at lower values of bentonite corrosion resistance get reduced. Furthermore, corrosion resistance is also associated with the formation of delayed ettringite formation(DEF)(P.K. Mehta, 2006) as a result of reaction of sulphuric acid with free lime. For control bricks the weight loss is higher due to more available amount of free lime, which get reduced steadily for incremental bentonite incorporated brick composite. Therefore, from supplementary analysis(XRD, FTIR and TGA) free lime availability get reduced with the incorporation of bentonite. Moreover, weight loss of compressed brick decreased along replacement of clay with bentonite due to resistance to moisture penetration(H. Komine, 1999) and higher ion exchange capability(Dixon, 1985) of the bentonite, for these intrinsic attributes bentonite is used in nuclear waste disposal system(Dixon, 1985; H. Komine, 1999). Moreover, densified microstructure and fewer quantity of calcium hydroxide in bentonite rich composites increased the its sulphate resistance(J. Mirza, 2009; S . AHMAD 2011). Hence, sulphate resistance of compressed bricks

increased with bentonite inclusion. Therefore, detailed durability investigation is needed for long term exposure of bricks to harsh environment.

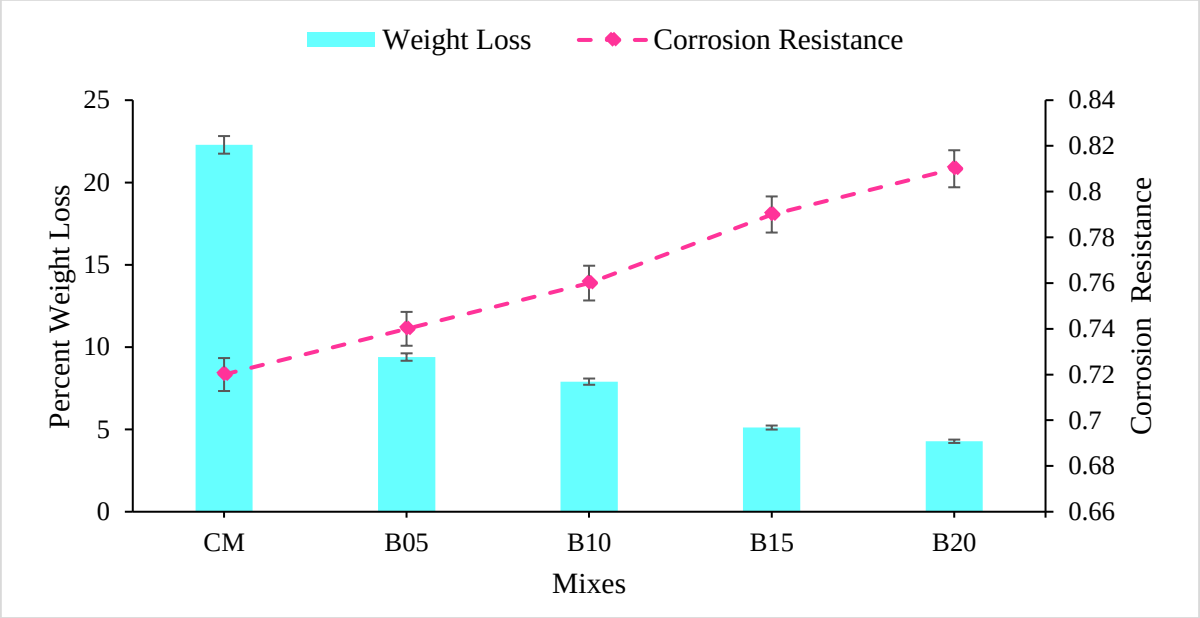


Figure 4-18: Sulphate resistance of lime-bentonite clay brick composite

## Chapter 5

# Conclusions and Recommendations

In this research, sustainable and eco-friendly incorporation of bentonite in lime stabilized compressed clay brick was suggested. Following conclusions were drawn based on the results and observations.

1. Material characterization results revealed that bentonite satisfied the chemical and physical requirement of pozzolan, whereas quick lime act as an alkaline activator for initiating geo-polymerization reaction. The average particle size of the lime bentonite clay composites decreased due to finer particle size of bentonite. The plasticity of lime-bentonite clay composite increased due to higher adsorbing capability of the bentonite. Optimum moisture content of the composite increased due to higher interlayer absorption characteristics of bentonite with the decreasing values of associated hardened density attributed to the swelling of bentonite.
2. Physico-mechanical properties of lime-bentonite compressed clay bricks classified as building bricks for negligible weathering according to ASTM standard C62-13. Water absorption of unfired, fired and compressed bricks decreased due to densification of microstructure by geo-polymerization reaction, sintering of clay minerals, voids reduction by swelling and pozzolanic activity respectively. Generally, unit weight of bricks reduced for increasing bentonite replacement for all brick types. Therefore, compressed bricks can be used for structural purpose in negligible weathering condition.
3. Microstructural analysis of the compressed clay bricks revealed the densified, bright and featureless hydration products with the incremental bentonite content as evidenced from calcium to silica ratios obtained in EDX. Void reduction observed due to physically applied compression, geo-polymerization reaction and formation of pozzolanic hydrates.
4. Supplementary analysis including X-ray diffraction, Fourier transform infrared spectroscopy and thermogravimetric of compressed and unfired bricks revealed the increased formation of calcium silicate hydrate, calcium aluminate hydrate and reduced portlandite content by increasing bentonite content for unfired bricks, whereas, increased calcium silicate hydrate formation in bentonite rich composite with reduced portlandite content. Hence, geo-polymerization is significantly evident in unfired bricks due to higher mixing water content and pozzolanic reaction in compressed bricks.

5. Thermal conductivity of compressed bricks reduced with the increasing replacement of bentonite with clay due to swelling characteristics attributed to the osmotic pressure generated by the interlayered water. Thermal conductivity of brick reduced from 0.51 to 0.38, room prototype containing brick as structural members increased the reduction of cooling load and decreased carbon emissions to 15.45%, ensuring the energy efficiency, sustainable and eco-friendly options against fired bricks.
6. Sulphate resistance of compressed bricks revealed the increased corrosion resistance and weight gain with added bentonite content. The maximum corrosion resistance and minimum weight loss values were recorded as 0.81 and 4.27% respectively for B20. Therefore, sulphate resistance of compressed bricks increased with bentonite inclusion.

Since, compressed brick produced encompasses the lower carbon foot prints during its manufacturing, structurally adequate and provides an energy efficient solutions to the conventionally fired bricks due to reduction in cooling loads. Lime-bentonite compressed clay bricks are energy efficient and satisfied structural requirements, therefore, can be used as an alternative to conventional bricks.

# References


1. A. Mohamed Musthafa, K.J., G. Velraj 2010. Microscopy, porosimetry and chemical analysis to estimate the fi ring temperature of some archaeological pottery shreds from India. Microchemical Journal 95, 311–314.
2. Ahmari S, Z.L., 2012. Production of eco-friendly bricks from copper mine tailings through geopolymerization. Constr Build Mater 29, 323–331.
3. Alaa Shakir, A.M., 2015. Durability property of fly ash, quarry dust and billet scale bricks. Journal of Engineering Science and Technology 10(5), 591 - 605.
4. Alaa A. Shakir, S.N., Kamal Nasharuddin Mustapha, 2013. Properties of bricks made using fly ash, quarry dust and billet scale, quarry dust and billet scale. Constr. Build. Mater. 41, 131–138.
5. Arioz O, K.K., Tuncan M, Tuncan A, Kavas T., 2010. Physical, mechanical and microstructure properties of F type fly ash based geopolymer bricks produced by pressure forming process. . Adv Sci Technol 21, 69–74.
6. ASTM, 2017a. Road and pavement materials, Standard Test Method for Particle-Size Distribution (Gradation) of Fine-Grained Soils Using the Sedimentation (Hydrometer) Analysis.
7. ASTM, 2017b. Standard Test Methods for Liquid Limit, Plastic Limit, and Plasticity Index of Soils1, D4318 − 17.
8. ASTM, 2013. Standard Specification for Building Brick (Solid Masonry Units Made From Clay or Shale).
9. ASTM C177-13, 2013,. Standard Test Method for Steady-State Heat Flux Measurements and Thermal Transmission Properties by Means of the Guarded-Hot-Plate Apparatus,. ASTM International, .
10. ASTM., 2017. Standard Specification for Coal Fly Ash and Raw or Calcined Natural Pozzolan for Use in Concrete, C618. West Conshohocken, USA.
11. Bell, F.G., 1996. Lime stabilisation of clay minerals and soils. Engineering Geology 42, 223 – 237.
12. Bilgin N, Y.H., Arslan S, Bilgin A, Günay E, Marsoglu M. , 2012. Use of waste marble powder in brick industry. . Constr Build Mater 29, 449–457.
13. Boardman, D.I., Glendinning, S., Rogers, C.D., 2001. Development of stabilisation and solidi fication in lime-clay mixes. Géotechnique 50, 533 –543.
14. Borgwardt, R.H., 1989. Sintering of nascent calcium oxide. Chemical Engineering Science 44(1), 53-60.
15. Brandl, H., 1981. Alteration of soil parameters by stabilisation with lime, Proceeding of 10th International Conference in Soil Mechanics and Foundation Engineering. A.A. Balkema, Stockholm, pp. 587 –594.
16. Building Code of Pakistan 2007. National Engineering Services of Pakistan, Seismic Hazard Evaluation Studies. Ministry of Housing and Works, Government of Pakistan, .
17. Chen C, L.Q., Shen L, Zhai J., 2012. Feasibility of manufacturing geopolymer bricks using circulating fluidized bed combustion bottom ash. Environ Technol 33(11), 1313–1321.
18. Chen, J., et al., 2017. A review of biomass burning: Emissions and impacts on air quality, health and climate in China. Science of the Total Environment 579, 1000-1034.
19. De Vries, D.A., 1963. Thermal properties of soils, Physics of Plant Environment, North-Holland Publishing
20. Company, Amsterdam. Journal of royal meteorological department society, 210–235.
21. DIN, 2012. Clay Masonry units with Specific Properties. pp. 105-100.
22. Dixon, D.A.a.W., D.R., , 1985. Physical Properties and Standards for Testing Reference Buffer Materials. Atomic Energy of Canada Limited Technical Record.

23. E. Vitale , D.D., M. Paris, G. Russo, 2017. Multi-scale analysis and time evolution of pozzolanic activity of lime treated clays. Applied Clay Science 141, 36 –45.
24. Faria KCP, G.R., Holanda JNF. ;:, 2012. Recycling of sugarcane bagasse ash waste in the production of clay bricks. J Environ Manage 101, 7–12.
25. Francisca Santiago, A.E.M., Mónica Osorio, Carlos Rivera, 2007. Preparation of composites and nanocomposites based on bentonite and poly(sodium acrylate). Effect of amount of bentonite on the swelling behaviour. European Polymer Journal 43(1), 1-9.
26. Freidin, 2007. Cementless pressed blocks from waste products of coal-firing power station. Constr Build Mater 21, 12–18.
27. Gao, S., et al., 2003. Water-soluble organic components in aerosols associated with savanna fires in southern Africa: Identification, evolution, and distribution. Journal of Geophysical Research: Atmospheres 108(D13).
28. García-Lodeiro, C.F.Z., A. Fernández-Jimenez A. Palomo 2105. The role of aluminium in alkali-activated bentonites. Materials and Structures 48(3), 585–597.
29. Glenn, G.R., Handy, R.L., 1963. Lime clay mineral reaction products. . Highway Research Record 29, 70 –82.
30. H. Komine, N.O., 1999. Experimentall study on swelling characteristics of sand-bentonite mixture for nuclear waste disposal. Soil and Foundation 39(2).
31. Haiying Z, Y.Z., Jingyu Q. . , 2011. Utilization of municipal solid waste incineration (MSWI) fly ash in ceramic brick: product characterization and environmental toxicity. Waste Management (Oxford) 31, 331–341.
32. Han, Y., 2017. Advances in energy and environmetal materials, Procedding of Chinese Materials conference. Springer, China.
33. Hayati-Ashtiani, M., 2013. Characterization of Nano-Porous Bentonite (Montmorillonite) Particles using FTIR and BET-BJH Analyses. Particle system characterization.
34. Hewlett, P., 2004. Lea's Chemistry of Cement and Concrete. Elsevier Science & Technology Books.
35. Ingles, O.G., and John B. Metcalf., 1972. Soil stabilization principles and practice. 11.
36. Institute, B.S., 1990. Stabilised Materials for Civil Engineering Purposes, Part 2: Methods of Test for Cement-stabilised and Lime-stabilised Materials.
37. J. Mirza, M.R., A. Naseer, F. Rehman, A.N. Khan, Q. Ali, 2009. Pakistani bentonite in mortars and concrete as low cost construction material. Applied Clay Science 45, 220-226.
38. J.M. Perez, M.R., 2014. Microstructure and technological properties of porcelain stoneware tiles moulded at different pressures and thicknesses. Ceramics International 40, 1365–1377.
39. James, R., Kamruzzaman, A.H., Haque, A., 2008. Behaviour of lime-slagtreated clay, Proceedings of the ICE-Ground Improv. . Wilkinson, pp. 207 –216.
40. Johansen, O., 1975. Thermal conductivity of soils. Trondheim, Norway.
41. Kae Long Lin, 2006. Feasibility study of using brick made from municipal solid waste incinerator fly ash slag. Journal of Hazardous Materials, 1810–1816.
42. Kumar A, K.S., 2013. Development of paving blocks from synergistic use of redmud and fly ash using geopolymerization. . Constr Build Mater 38, 865–871.
43. Kumar, R., Aggarwal, R.K., Gupta, D., Sharma, J.D., 2013, 2013. Carbon emissions from airconditioning. J. Eng. Res. 02, 72-74.
44. L. Vorrada, P.T., K. Kanyarat, S. Chatnarong, 2009. Effects of recycled glass substitution on the physical and mechanical properties of clay bricks. Journal of Waste Management 29, 2717–2721.
45. Lee, B.-J., et al., 2014. Air Pollution Exposure and Cardiovascular Disease. Toxicological Research 30((2)), 71–75. .
46. Little, D.N.s., 1996. Fundamentals of the Stabilization of Soil With Lime. National Lime Association. , Arlington, USA,, pp. 1 –20

47. M. Shahul Hameed, A.S.S.S., 2009. Properties of green concrete containing quarry rock dust and marble sludge powder as fine aggregate. Asian J. Eng. Appl. Sci. 4, 83–89.
48. Mezencevova A, Y.N., Burns SE, Kahn LF, Kurtis KE., 2012. Utilization of Savannah harbor river sediment as the primary raw material in production of fired brick. . J Environ Manage 113, 128–136.
49. Mohan NV, S.P., Rao KS, 2012. Performance of rice husk ash bricks. Int J Eng Res Appl 2(5), 1906–1910.
50. Nehdi M, D.J., Damatty AE, 2003. Performance of rice husk ash produced using a new technology as a mineral admixture in concrete. cement Concrete Resources(33), 1203-1210.
51. Oti, J.E., 2010. The Development of Unfired Clay Building Materials for Sustainable Building Construction. University of Glamorgan, UK.
52. P.K. Mehta, P.J.M.M., 2006. Concrete: Microstructure, Properties and Materials. McGraw-Hill, USA.
53. Peters T, I.R., 1978. Mineral changes during firing of calcium-rich brick clays. Ceramic Bulletin 57(5), 503 – 509.
54. Quijorna N, C.A., Andres A, Cheeseman C. , 2012. Recycling of Waelz slag and waste foundry sand in red clay bricks. Resour Conserv Recycl 65, 1–10.
55. Rahman, 1987. Properties of clay–sand–rice husk ash mixed bricks. . International Journal of Cement Composite and Lightweight Concrete 9(2), 105-108.
56. Raut S, R.R., Mandavgane S, 20013. Utilization of recycle paper mill residue and rice husk ash in production of light weight bricks. CIvil Architecture and Mechanical Eng(13), 269-275.
57. Reddy BVV, J.K., 2003. Embodied energy of common and alternative building materials and technologies. Energy Build 35, 129–137.
58. Robert Levy, P.P., 2017. World of Change: Global Temperatures. (Accessed 2 feb, 2019 2019).
59. Robinson, G., 1982. Characterization of bricks and their resistance to deterioration mechanisms. Conservation of Historic Stone Buildings and Monuments,, 145-162.
60. Roger J. Cheng, J.R.H., Jung T. Kim, Show-Mei Leu, 1987. Deterioration of Marble Structures. ANALYTICAL CHEMISTRY 59.
61. Roman, P., 2014. A Brief History of Ceramic Innovation. In: An Introduction to Ceramics, in: Springer, C. (Ed.) Lecture Notes in Chemistry.
62. S . AHMAD , S.A.B., A. ELAHI, J. IQBAL, 2011. Effect of Pakistani bentonite on properties of mortar and concrete. Clay Minerals 46, 85–92.
63. S. A. Memon, U.J., R. A. Khushnood, 2019. Eco-friendly utilization of corncob ash as partial replacement of sand in concrete. Construction and Building Materials 195, 165–177.
64. S. B. pally, C.C., D. N. Arnepalli, 2017. Characterization of Lime-Treated Bentonite Using Thermogravimetric Analysis for Assessing its Short-Term Strength Behaviour. Indian Geotech J.
65. SAARC, 2012. Evaluating Energy Conservation Potential of Brick Kilns in SAARC Countries. Islamabad, Pakistan.
66. Sengupta P, S.N., Borthakur PC., 2002. Bricks from petroleum effluent treatment plant sludge: properties and environmental characteristics. J Environ Eng 128(11), 1090–1094.
67. Shamiso Masuka, W.G.a.T.R., 2018. Development, Engineering Properties and Potential Applications of Unfired Earth Bricks Reinforced by Coal Fly Ash, Lime and Wood Aggregates. Journal ofBuilding Engineering.
68. Sherwood, P.T., 1993. State of the art review-Soil Stabilization with Cement and Lime., London.
69. Standards, E., 2005. Specification for Masonry Units-Part 1, clay masonry units.
70. Stutzxnan, P.E., & Centeno, L., 1995. Compositional analysis of beneficiated fly ashes. National Institute of Standards and Technology Interagency Report, USA.

71. Sudhakar Rao, M., Shivananda, P., 2005. Role of curing temperature in progress of limesoil reactions. Geotech. Geol. Eng. 23, 79 –85.
72. Surendra Roy, G.R.A., Rama N. Gupta, 2007. Use of gold mill tailings in making bricks: a feasibility study. Waste Management & reearch 25(5).
73. Sutcu M, A.S., 2009. The use of recycled paper processing residue in making porous brick with reduced thermal conductivity. Ceram Int 35, 2625–2631
74. Syed M.S. Kazmi, S.A., Muhammad. Saleem a, Muhammad J. Munir b, Anwar Khitab, 2016. Manufacturing of sustainable clay bricks: Utilization of waste sugarcane bagasse and rice husk ashes. Construction and Building Materials 120, 29–41.
75. Tremblay, H., Leroueil, S., Locat, J., 2001. Mechanical improvement and vertical yield stress prediction of clayey soil from eastern Canada treated with lime or cement. Canadian Geotechical Journal 38, 567 –579.
76. Wisal Ahmed, R.A.K., Shazim Ali Memon, Sajjad Ahmad, Waqas Latif Baloch, Muhammad Usman, 2018 Effective use of sawdust for the production of eco-friendly and thermal-energ y efficient normal weight and lightweight concretes with tailored fracture properties. Journal of Cleaner Production 184, 1016-1027.
77. X. Lingling, G.W., W. Tao, Y. Nanru,, 2004. Study on fired bricks with replacing clay by fly ash in high volume ratio. Construction and Building Materials 19, 243–247.
78. Y. Maniatis, M.S.T., 1981. Technological Examination of Neolothic-Bronze and Age Pottery from Central and South Europe and from the Near East. Journal of Archaeological Science 8, 59-76.
79. Yazici, 2007. The effect of curing conditions on compressive strength of ultra high strength concrete with high volume mineral admixtures. Build Environ 42, 2083–2089.
80. Zain MFM, I.M., Mahmud F, Jamil M., 2011. Production of rice husk ash for use in concrete as a supplementary cementitious material. Construction and Buiding Materials(25), 798-805.
81. Zhang, 2014. Production of bricks from waste materials – a review. Constr Build Mater 47, 643–655.
82. Zhang, H., et al., 2016. Air pollution and control action in Beijing. Journal of Cleaner Production 112, 1519-1527.